OPTICAL CHARACTERIZATION OF THIN FILM SOLAR CELLS

A THESIS SUBMITTED TO
THE SCHOOL OF GRADUATE STUDIES
ADDIS ABABA UNIVERSITY

IN PARTIAL FULFILLMENT OF THE
REQUIREMENTS FOR THE DEGREE OF
MASTER OF SCIENCE IN PHYSICS

BY

ENDESHAW BEKELE
ADDIS ABABA, ETHIOPIA
JUNE, 1996

ADDIS ABABA UNIVERSITY

SCHOOL OF GRADUATE STUDIES

OPTICAL CHARACTERIZATION

OF

THIN FILM SOLAR CELLS

BY

ENDESHAW BEKELE

DEPARTEMENT OF PHYSICS

FACULITY OF SCIENCE

ADDIS ABABA UNIVERSITY

ADDIS ABABA UNIVERSITY

SCHOOL OF GRADUATE STUDIES

OPTICAL CHARACTERIZATION OF THIN FILM SOLAR CELLS

By

Endeshaw Bekele
Department of Physics
Faculty of Science

Approved by the Examining Board:

Prof. Thomas Wicher, Ext. Examiner

Dr. U. Stutenbaumer, Advisor

Prof. R.Y. Thakur, Examiner

ACKNOWLEDGMENT

I would like to express my heart felt gratitude to my advisor Dr. Ulf Stutenbaumer for his consistent advise, unreserved guidance, with kind heart and full patience encouragement throughout the work. I have no words to thank him for his guidance in using computers and his cooperation even to use his own PC in facilitating the work.

I extend my warmest gratitude to the solar cell technology group (Dr. Claus Beneking) at the institute for Thin Film and Ion Technique photovoltaic (ISI- PV), KFA- Juelich, Germany for preparing the samples and Dr.Th. Eickoff for his good cooperativeness to send them. Besides it is my pleasure to acknowledge him gratefully for his kind cooperation in taking his time to read my thesis work and give very valuable comments.

I am grateful to all members of the Physics Department of the AAU who have delivered their unreserved help throughout my stay. In particular, Ato Tadesse Tasew for his help in facilitating the work and Ato Challa Bekele for his cooperativeness in giving me his data on Reflectance and Transmittance measurements which has been done previously on the samples.

I wish to thank the Ministry of Education who granted me sponsorship to participate in the graduate program and in particular Ato Belay Wondimu for his kind help. I am also thankful to the school of graduate studies and Physics Department of the AAU for their material support.

It is my pleasure to thank my friends in Debre Brehane and Addis Ababa for their help and encouragement throughout my study.

Finally, thank God for what is done to start and complete my study.

CONTENTS Page

List of Tables **Page**

List of Figures **Page**

ABSTRACT

The optical properties of glow discharge (GD) produced p-, i-, and n- layers of hydrogenated amorphous Silicon a - Si : H, thin films have been investigated over a wide photon energy range 1.24 eV < E < 3.54 eV using room temperature reflectance (R) and transmittance (T) measurements. The data is compared with room temperature R and T measurements done on the same samples in the laboratory of ISI - PV in Forschungszentrum, Juelich, Germany over an energy range of 1.13 eV < E < 4.13 eV. The similarities and differences between individual R and T measurements done in the two laboratories and optical functions deduced from the measurements are discussed. A common value for the optical energy gap within the value (up to $\pm$ 0.04 eV) is obtained. As a solar cell component, the investigated sample p- layer does not harvest effectively photons from the visible sunlight energy spectrum. The possibility of the measurement of optical constants in the Addis Ababa University Department of Physics is verified for the first time.

1. INTRODUCTION

Solar energy, which is clean and practically unlimited, is expected to be a desirable alternate energy source to conventional power supplies, and demand for the photovoltaic systems has increased throughout the world, especially in Europe and in the United states. In developing countries such as in Ethiopia, environmental pollution from modern technology is not as such what to be afraid of (at least for the time being). But the need for direct electrical output in remote areas where the settelement is in scattered habitation consisting of a number of huts necessitates the need for the solar energy resource. This is the case, for example, where rural electrification, telecommunication, water pumping, irrigation, etc., is needed.

Photovoltaic(PV) cells or solar cells are probabily the most effective method for capturing solar energy, since they are easy to use and are the most effective means of directly generating electricity.

A PV system is a modular, fully solid state electricity generator. Its electrical output can be engineered virtually for any applications, varying from wrist watch and calculators to solar home systems and generating power at electric utility stations [13,27]. The need for PV is expected to expand enormously when electricity from it can be feed in to electricity stations at costs that are comparable to generation cost of electricity from other sources. This can be done if the total PV systems costs are reduced significantly [27].

For this reason scientists and engineers throughout the world are working on the development of PVsystems with a better cost / performance ratio. This is done by increasing the efficiency of cells and modules, by reducing their cost or both. Apart from technological improvement, scaling up of production is a pre- requisite for realizing low cost.

As it is elsewhere [1 - 29] stated the knowledge of optical constants of a film from a given material is of a basic importance in determining the characteristics of light

transmission and hence in designing devices such as solar cells. The basic method for calculating the optical constants of a thin film in which interference phenomena can be observed when it is exposed to light consists of refering to reflectance and transmittance measurements from which optical parameters such as refractive index, absorption coefficient, extinction coefficient, optical enegy gap can be determined.

The need for the optical measurement set up, to learn the method of determining the optical constants and promoting the knowledge for the use is unquestionable. Optical characterization of thin films for solar cell use have started in Addis Ababa University Department of Physics for the first time. To start with, measurements are done on the samples which are already investigated by Ato Challa Bekele in the laboratory of ISI - PV in Forschungszentrum, Juelich (Germany).

From the reflectance and transmittance measurements done at room temperature the optical functions for the glow discharge produced hydrogenated amorphous silicon a- Si : H, thin films have been obtained over the energy range 1.24 eV < E < 3.54 eV. In this thesis work, the room temperature measurements done on these samples over the energy range between 1.13 eV and 4.13 eV in the Juelich laboratory are presented for comparison.

2. THIN FILM SEMICONDUCTORS

2.1 Amorphous Silicon Thin Film Semiconductors

2.1.1 General

A material can empirically be defined to be amorphous if its x- ray diffraction pattern consists of diffused rings or (halos) rather than sharply defined Bragg rings or spots which are characteristics of polycrystalline or single crystals [2].

Amorphous semiconductors, silicon (Si) and the others, are metastable thin solid film materials [1,2]. They are solids in their internal equilibrium in which there is, just as in the crystalline solids, a definite set of equilibrium positions about which the atoms oscillate. But in contrast to the crystalline solids the environment of each atom doesn't repeat itself in precise periodicity. It differs from site to site ultimately leading to the loss of the long- range order translational periodicity of their constituent atoms. Hence there exist a disorder which is inherited in them. With disorder it means there will unavoidably be atoms with local configurations such as, stretched or compressed bond lengths and distorted bond angles. This gives rise to tail states [1, 3] to the valence band and conduction band structures (i.e. extended states) which are generally similar to that of the crystalline solids except for some deep states, sharpened upper edge of the valence band and relatively featureless appearance of the conduction band [3]. There are also errors in co-ordination which are intrinsic and extrinsic to the amorphous solids. These are atoms whose nearest neighbour is not satisfied according to their chemical valency. The intrinsic ones are for instance, Si atoms bonded to only three of their nearest atoms instead of four giving rise to " unfilled " or dangling bonds and hence defect states or traps which are deep below the tail states [3-5]. The addition of foreign atoms also introduces additional deep defect states.

Both the tail states and defect related states lead to the major distinguishing feature of a-Si. The continuum of localized states, in which a charge carrier occupying them, has therefore

no chance of moving away or it is getting trapped (zero mobility) in the energy range is termed as mobility gap. This has an influence on their optical properties.

2.1.2 Mobility Gap

The energy band gap of the crystalline counter part is replaced by an energy range in which there are localized states typically with the order in the range between (10^{-3} - 10^{-7}) of the number of states in one of the extended state bands (10^{22} cm^{-3} eV^{-1}) [4]. Even though it sounds a very small fraction it has an influence on the quality of the material. Localized as well as non localized states can exists within the same band, the demarcation being the conduction and the valence band edges. Different band models have been proposed to show the distribution of these states [1,12] . The figure below (Fig. 2.1) shows one of the models, proposed by Mott and Davis in 1968.

The mobility gap μ_g, is generally smaller than the optical band gap of the a-Si while its crystalline counter part, the forbidden gap is equal to the optical band gap of the crystalline silicon [1,12].

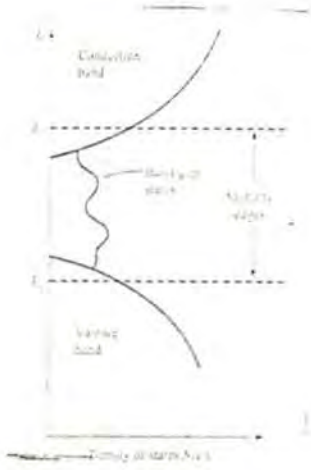

Fig. 2.1 Band model of a non crystalline semiconductor. E_v and E_c are the mobility edges of the valence band and of the conduction band, respectively.

2.1.3 Density of States

The determination of density of states (DOS) structure of a given material generally requires a knowledge of the atomic structure , the phonon structure, and the derivation of the excited electronic structure. This is more difficult for amorphous silicon because of the absence of the long-range order periodicity [1]. Several factors such as the interatomic distances, the co-ordination number, and the type of the chemical bonding determine the DOS for a given material.

Energy band theory has relied on the derivation of the E (K) relation ship. In this treatment, the concept of periodicity is vital. Periodicity asserts that only the primitive unit cell needs to be considered. This is the approximation which can aid to solve the problem of the DOS determination in crystalline silicon (C-Si) based on translational symmetry. However, the short-range order is apparently more important than the lack of the long-range order, since several factors as the interatomic distances, the co-ordination number and the type of chemical bonding determine the DOS of a given material [1]. The distribution of deep localized states has been more controversial. Part of the reason is that the deep state density is much more sensitive to the details of the deposition, and so there are real differences in the samples made under different conditions. The typical value reported is on the order of $10^{15}cm^{-3}\ eV^{-1}$ to $10^{17}cm^{-3}eV^{-1}$ [4].

2.1.4 Preparation of a-Si Thin Films

Films of amorphous silicon prepared by reactive sputtering or evaporation revealed that the density of the localized states in the mobility gap was far too high to be of any use in device application [1,2].

By introducing hydrogen into the evaporated or into the sputtered films, either during the preparation or the subsequent infusion of atomic hydrogen, it is possible to reduce the

density of the localized states. Deposition of Si by plasma enhanced chemical vapor deposition (PECVD) or glow discharge (GD) from silane SiH_4, gas has a similar effect if the temperature of the deposition is low ($\leq$ 400 $^{\circ}C$).

It was found that the hydrogen concentration in hydrogenated amorphous silicon a-Si : H can be as high as 40 % -50 % depending on the deposition conditions [2]. However, "device quality" a-Si : H materials generally have an hydrogen concentration of less than 10 % [1,2].

2.1.5 Hydrogenation of a-Si Thin Films

Amorphous silicon when nominally pure has dangling bonds. It is the accidental discovery by researchers at the Standard Telephone Laboratory and University of Dundee in the U.K. in the early 1970's revealed that the GD or PECVD deposited a-Si thin films prepared from silane gas possessed a low DOS [1,2]. Subsequently it was discovered that these films contained approximately 10 atomic percent hydrogen and hence appropriately refered as a-Si : H type alloys.

Here hydrogen takes the opportunity of pairing the dangling Si bonds which cannot be paired to each other. Other atoms e.g., oxygen, nitrogen, fluorine, etc., may aid also in the passivation process. The addition of H and subsequent removal of dangling bonds is provided by various indirect measurements. The peak in the photoluminesence spectrum will shift to higher energies (1.35 eV) as the DOS is reduced [2,9], while unhydrogenated materials show a much reduced luminescence peak at lower energies. Addition of hydrogen enlarges the band gap besides the passivation of the gap states.

2.1.6 Doped a- Si Thin Films

The possibility of substitutional doping in crystalline semiconductors, has been one of the most important factors in the development of semiconductor physics. Semiconductors can conduct electricity if free carriers are introduced into the conduction band. One way of doing this is by doping the semiconductor with impurities [12].

The lack of a similar sensitive control in the case of amorphous semiconductors had been a serious limitation in this field. The presence of a continuum of localized states throughout the mobility gap has the effect that the doping fills localized states with electrons or holes. Only part of the impurity atoms are built in the network as substitutional or interstitial donors or acceptors [2].

Generally, n- and p- type doping is achieved by the addition of phosphine, PH_3 and di-borane (6), B_2H_6 gas to SiH_4 in the gas phase, respectively. Doping creates extra defect states within the mobility gap.

2.2 a-Si Solar Cells

Solar cell operation is based on the ability of the semiconductor to convert sunlight directly into electricity by exploiting the photovoltaic effect. In the conversion process, the incident energy of light creates hole-electron pairs in the semiconductor which are then separated by the device structure and afterwards collected by contacting electrodes to produce an electric current [12].

Semiconductor materials used to fabricate solar cells are sensitive to the color of the sunlight. Certain materials absorb sunlight more effectively than others [11-13]. Amorphous silicon is among the efficient absorbers. Thus only thin layers of such materials are needed to produce the same amount of electric power that a thicker layer of material such as

crystalline silicon would produce. A thickness ratio of about 500 : 1 for crystalline silicon compared to amorphous silicon (a-Si) is observed [13].

Sunlight consists of a continuum of colors or wavelengths. Much of it will be either too low in energy to produce free electrons and holes or will be too energetic and thus produce only wasteful heat in the material [13]. For example, for crystalline silicon with a band gap of 1.12 eV, the light energy corresponding to the long wavelength cut-off and short wavelength cut-off are respectively 1.13 eV and 3.1eV [8,13].

Hydrogenated amorphous silicon thin films produced from glow discharge of silane are relatively efficient solar cell components [1,5,9,10]. Among the positive conditions are:

a) A high absorption coefficient ($> 10^5 cm^{-1}$) over the visible spectrum (1.8 eV - 3 eV) making submicron (of the order 0.6 μm [9]) thick devices practical and economical [10].

b) It can be deposited on any inexpensive substrates which needs only to be heated to a relatively low temperature ($< 200\ ^{0}C$ - $300\ ^{0}C$) [2] e.g., glass [5].

c) The necessary conductivity can be obtained by doping substitutional impurity atoms. The structure sensitivity in a-Si : H type alloys enables the possibility to develop the p- i- n junction devices similar to that formed from the crystalline silicon [5].

d) It is easy to produce alloys with other group IV elements allowing the optical gap to be raised or to be lowered [8].

2.2.1 p- n and p- i- n Structure Solar Cells

Both p- and n- materials of amorphous silicon have poor transport properties compared to that of single crystalline silicon and the simple p- n junction solar cells have a low efficiency (12.7 %) compared to a crystalline silicon p- n structure solar cells (23 %) [14].

Because of the low effective mobilities of the electrons ($\mu_e \sim 10^1 cm^2 s^{-1} V^{-1}$) and the holes ($\mu_h \sim 1\ cm^2 s^{-1} V^{-1}$) of a-Si as compared to that of electrons ($\mu_e \sim 1500\ cm^2 s^{-1} V^{-1}$) and the holes ($\mu_h \sim 500\ cm^2 s^{-1} V^{-1}$) in the C-Si, the most important carrier generation of charge carriers in the a-Si is limited to absorption that occurs within the space charge region. The width of this space charge region is linked to the DOS spectra. The lower the DOS the larger will be the width of the space charge region and hence the collection region. Doping creates extra states with in the energy gap leading to a decrease in the overall collection width [9]. Therefore, this simple solar cell structure is ruled out for use.

Instead of p-n type devices intrinsic amorphous silicon is inserted to improve the transport properties, the charge separation is now occurring within the intrinsic layer and the basic requirement is that the p- and the n- layers should be thick enough to sustain the depletion width [9, 15]. The development of p- i- n junction cells led to a rapid improvement in the performance of solar cells.

Heavily doped p- layers (p^+) can be formed with addition of B_2H_6 to SiH_4 gas. However this is accompanied by a reduction in the optical band gap. Therefore, for a solar cell illuminated through the p^+- layer there will be a loss in the photogeneration at the blue end of the spectrum.

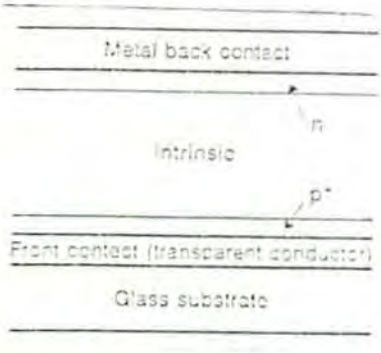

Fig. 2.2 p- i -n solar cell structure [15].

To avoid this loss, wide gap (1.76 eV - 2.2 eV) amorphous materials composed of Si C B H has been developed and used [9, 22]. An i- layer which is not in fact completely intrinsic but which is slightly n- type is used [13]. For light entering a cell through a sufficiently thin heavily doped p- layer, so that only little of the light is absorbed by it, there will be a maximum photogeneration of the charge carriers in the i- layer. Moreover, the electric field between the heavily doped p^+- layer and very slightly n- doped " i " layer is highest. It is therefore, in the region of maximum photogeneration, p^+/ i interface, there exists a sufficiently maximum electric field for the separation of the photogenerated charge carriers.

The optimum structure of the a-Si is then, the p^+- i- n structure, having a transparent contact to the p^+- layer and an ohmic contact to the n- layer.

2.2.2 Efficiency of Solar Cells

Sunlight absorbed by semiconductors is converted into DC electric power through relative increases in the potential energies of the minority carriers. The electron- hole pair generated upon absorption of photon gives rise to the relative increase in the concenteration of minority carriers. The concenteration gradient that exist will then exert a force on the mobile charged carriers in the neutral regions. This gradient force changes charged carrier potential energies with distance deep into neutral regions from the depletion region edge, by implcation with concentration of the minority carriers..

Electrons and holes have to be separated spatially and collected in order to use the energy that each pair represents. To achieve separation, the minority carriers have to diffuse or drift to the junction, where they will be swept away by the built in electric field to the regions where they become majority carriers. It is this majority carriers that ultimately flows through the two metal contacts to an external circuit. In open circuit condition, this process will

lead to a build up of a potential difference V_{oc} between the front and back contacts and in short circuit condtions to a current I_{sc} . The challenge is to convert the non-equilibrium minority carrier concentration in to majority carriers with as little loss of their added potential energy.

The short circuit current density J_{sc}, the open circuit voltage V_{oc}, and the fill- factor, FF constitute the three major solar cell parameters. These three are related to the solar cell efficiency η [11, 12, 20]. An efficient solar cell requires that the J_{sc} , V_{oc}, and the FF are all maximized. These parameters are interrelated through complex relationships involving the solar cell materials. Based on theoretical studies limiting solar cell performances have been predicted. These have provided helpful guidance for improving the performance and for assessing the potential benefits of using materials with other band gaps. A conversion efficiency between 6 % -19 % [9] has been estimated for amorphous silicon solar cells. These wide discrepancies in estimation arises mainly due to the difficulty that exists in formulating the exact transport behavior in these devices. Even though it is an unstablized result an achieved efficiency of 12.7 % is recentely reported [14].

Formally the cell voltage is determined by the band gap minus the quasi-Fermi level spacing from the band edges at the edges of the depletion region. Solar cell current is fundamentally limited, by quantum nature of light, to one collected electron-hole pair per incident photon energy greater than the band gap.

The band gap gives the maximum J_{sc} . It and the minority carrier concetration define the maximum V_{oc} , which then gives the FF. The performance of solar cells below the theoretical value can be separated into deficit in current, voltage and fillfactor. The first of this is due to imperfect quantum efficiency and non-zero reflection the second is due to low minority carrier concentrations, which may be caused due to both radiative and non-radiative recombinations and the third one is due to excess leakage currents.

2.3 Optical Properties of Solar Cells

2.3.1 Determination of Optical Parameters

Optical measurement constitutes the most important means of determining the band structures of thin film semiconductors. When a beam of light is incident on a thin film, the light reflected or transmitted by the thin film has a certain character which could be described by optical parameters such as refractive index n, absorption coefficient α , extinction coefficient k, and optical energy gap, E_g^{OPT}.

Measurement of certain quantities which characterize the reflected or the transmitted light beams enables to know these optical parameters and there knowledge helps in designing devices such as solar cells. Reflectance and transmittance which are defined as a ratio of the reflected light intensity to the incident light intensity and transmitted light intensity to the incident light intensity are the two important quantities which are generally measured [11,16].

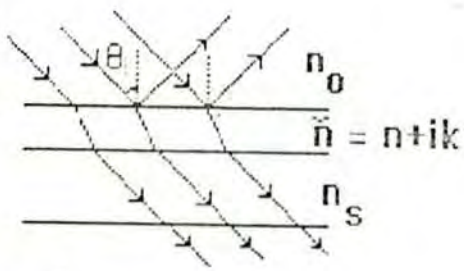

Fig. 2.3 Multiple interference by reflection or transmission of light through thin film layer on a thicker finite transparent substrate.

Consider a plane- parallel thin film of thickness d on a thicker transparent substrate on which a monochromatic light wave of wavelength λ is falling on its air / film interface at an angle θ_i . The substrate is assumed to be finite transparent and of negligible reflection.

In practice such a narrow beam cannot be used and the various reflected and transmitted component overlap each other. Interference of light rays will occur. Indeed, interference phenomena in the film occurs for a certain wavelength of light falling on the film for which there is no absorption and only the real part n, of the complex refractive index, $\bar{n} = n + ik$ is taken into account.

The successive interfering rays don't all have the same intensity because each successive reflection and transmission (interference from thin films can also be seen in the transmitted light) decreases its intensity. By adding up all the amplitudes, taking into account the relative phases of components the total reflectance and transmittance at normal incidence may be expressed as [17].

$$R = \frac{(n - n_o)^2 + k^2}{(n + n_o)^2 + k^2} \tag{2.1}$$

$$T \propto \frac{4n_o^2}{(n + n_o)^2 + k^2} \tag{2.2}$$

The film reflects two parallel beams of light rays. One of them was formed as a result of reflection from the air \ film interface and the second as a result of reflection from film \ substrate interface. The second beam is refracted when it enters the film. Part of it is transmitted through the substrate while part of it is reflected and again it gets refracted when it leaves the film before it meets the first beam. The path difference between the two reflected rays before they meet is [23]

$$\Delta s = 2d\sqrt{n^2 - \sin^2\theta_i} \tag{2.3}$$

where n is real part of the refractive index, θ_i is angle of incidence and it is zero for normal incidence.

In calculating the phase difference between the two successive reflected rays it is nece - ssary in addition to the optical path difference $\Delta\Sigma$, to take into account the possibility of the change in the phase of the wave up on reflection occurring from the interface between the optically less dense and optically denser medium and vice versa. A phase difference of π exists at the air / film interface and of zero at the film / substrate interface. Thus the condition for the interference maxima at the air / film interface will be the usual condition for the interference minima and vice versa. At normal incidence the conditions are [17,18] :

$$\Delta\Sigma = 2dn = (m + \tfrac{1}{2})\lambda \text{ , (maximum reflection, minimum transmission)} \qquad (2.4)$$

$$\Delta\Sigma = 2dn = m\lambda \text{ , (maximum transmission, minimum reflection)} \qquad (2.5)$$

where m is an integer and λ is the wavelength of the monochromatic light used to illuminate the film.

When white light is incident on the film, the reflected light can be dispersed using a spectrometer so that the wavelength at which maxima and minima occurs may be measured directly. This method enables thicker films to be dealt since the order of interference may be obtained from the position of the interference fringes in the resulting spectrum. Thick films show more maxima in the reflectance or transmittance spectrum than thin films.

Figure 2.3. b shows a transmission spectrum in the plane Fabry - Perot resonator see Fig. 2.3 a.) i.e. interference from transmission through two plane - parallel mirrors with constant separation distance or resonator length d.

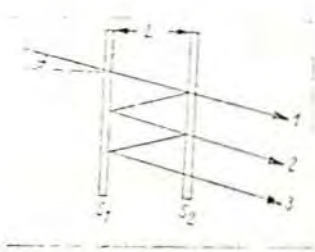

Fig. 2.3 [24,25] a) Plane Fabry- Perot resonator. b) Transmission in plane Fabry Perot resonator.

The optical path length between two successive transmission or reflectance maxima is known as free spectral range $\delta\nu$. When it is expressed in terms of wave number the equation is identical to the free spectral range of a grating monochromator [24]. Grating monochromators pass more than one order of diffracted light. That is, for any counter reading λ , the monochromator also transmits the wavelength λ / n , where n is an integer. If the n^{th} order of λ coincides with the $(n - 1)^{th}$ order of $\lambda + \Delta\lambda$, the wavelength band $\Delta\lambda$, describes the free spectral range [23,24].

$$\delta\nu = \frac{c}{\Delta\Sigma} \qquad (2.6)$$

where $c = 2.988 \times 10^{8} \frac{m}{s}$ is speed of light in vacuum

When the above expression is expressed in terms of energy and substituting $\Delta\Sigma$ from eqn. 2.5 at normal incidence $\delta\nu$ becomes [23] :

$$h\delta\nu = \frac{hc}{2dn} \qquad (2.7)$$

where $h = 6.626 \times 10^{-34}$ Js is Planck's constant.

The ratio of the free spectral range $\delta\nu$, to the full- width half- maximum (FWHM) $\Delta\nu$, of the spectral distribution of a single monochromatic line measures the fine-ness, or " finesse " of the fringes and the coefficient finesse N_f , for ideal plane - parallel mirror surface is defined by [24]

$$N_f \equiv \frac{\delta\nu}{\Delta\nu} \qquad (2.8)$$

The coefficient of finesse can be interpreted as the effective number of interfering beams. In a Fabry-Perot resonator the roughness of the mirrors as well as diffractional losses, which occurs with mirrors of finite length, reduces the total finesse.

2.3.2 Absorption Characteristics

An optical absorption in semiconducting material is usually observed for photon with energies greater or equal to their optical band gap energy. Here both the forbidden gap of C- Si and the mobility gap of the a-Si are taken to be equal to the optical band gaps of C-Si and a-Si respectively [3]. Photons with energy less than the optical band gap energy will only be transmitted through it without being absorbed. The fundamental optical absorption gives the measure of this optical band gap. But in a-Si semiconductor there is an optical absorption even for photons with energies less than the optical band gap energy. This give rise to a tailing, like that is seen in the extended states, to the fundamental absorption edge [3]. Again these appears to be related to the presence of localized states in the mobility gap [3, 9].

The inclusion of hydrogen to remove dangling bonds will decrease the optical absorption below the fundamental edge. But this is not directly related to the hydrogen concentration rather it is related to the presence of dangling bonds [2]. This hydrogen inclusion has also an effect of removing states from the top of the valence band and thus increasing the optical band gap.

Both a-Si and C-Si can absorb all the visible light spectrum. However, the optical absorption coefficient, which describes the relative number of photons absorbed per unit distance by the semiconducting material is more than an order of magnitude larger than that of C-Si over the most of the visible light range [4,12]. Thus most of the solar radiation with wavelength less than 0.7 μm can be absorbed within approximately 1 μm thick film of a- Si : H [9]. The absorption coefficient for photon energies near the band gap is usually determined from R and T measurements by using Hishikawa's relation which removes interference effects from the absorption spectra [16,30].

$$\alpha = -1/d \ \ln (T/ 1\text{-}R) \qquad (2.9)$$

where d is the thickness of the single thin film layer.

3. Experimental Set Up

In this chapter, all the experimental apparatus which has been used are listed, described, and the procedures are briefly described.

3.1 Experimental Apparatus

Every arrangement out of optical components requires a mounting structure in addition to light sources, spectral instruments and other optical components. The optical bench used was a traditional piece 158.8 cm long with 11 cm width and 15 cm height. Five of the mounts can be moved and fixed along its length while two of them can also be moved and fixed transversally.

R and T measurements on the samples over illumination spot size of ~ 10.4 mm^2 were performed using a Spex Minimate-2 Model 1681 B Spectro- meter with internal step drive circuitry that couples directly to a computer. Other components used with it are :

(1) Halogen lamp rated to 130 w. It has an aperture of 18 mm diameter.

(2) Power supply for halogen lamp performing the current stabilization.

(3) Lenses.

Two bi/ convex lenses of 50 mm focal length with diameters of 50 mm and 38 mm. Two bi/convex lenses each of 71 mm diameter and with 150 mm focal length. One bi/ concave lens of 71 mm diameter with 100 mm focal length. Each lens is with a holder.

(4) Mirrors.

Three plane glass mirrors silvered at the back, with holders were used. Two of them are to ensure the near normal incidence reflectance measurement and the other is for the normalization of the reflectance measurement. All the mirrors were uncalibrated.

(5) LEYBOLD-HERAUS measuring amplifier D.

It is a dc current measuring amplifier which is in connection with a voltmeter as indicator is used for the measurement of voltage. It has an output range between 0.3 V and 3 V (max.10V). The current range selector on its front panel which is in the range 10^{-11}A - 10^{-6}A is used to adjust the current gain. The zero adjustment knob at its input is used to adjust for the background measurement.

(6) Model M- 4650 CR digital multimeter.

It is a four digits multimeter with AD-converter unit. A computer interface connection were used to input the voltage signal out of the measuring amplifier and feed to the computer storing our data.

(7) Detector.

A Si p-i-n photodiode with a plastic, home made housing. It has a sensitive area of $1mm^2$ with normalized detectivity of $D^* = 5 \times 10^{12} \frac{cm\sqrt{Hz}}{W}$. Its maximum sensitivity is at 850 nm.

(8) Samples.

The samples were p- and n- layers of an approximately 1000 nm thickness, intrinsic layers of 100 nm and 1000 nm thickness. The layers are of a-Si : H deposited in glow discharge method over corning glass of refractive index, n = 1.5. The glass sides were checked by refraction phenomena seen when a sharp pen is placed in front of it.

(9) PC computers to be loaded with software:

a) 232_SCAN.BAS spectrometer control program written in GWBASIC .

It is a support software supplied from the SPEX company. On command the spectrometer is made to scan the desired spectral range with a step drive system that is linear with wavelength. This spectral instrument, the SPEX spectrometer, is a stepper drive grating monochromator of mechanical range 30 nm - 1000 nm, reciprocal dispersion 0f 3.7 nm / mm, grating blaze 500 nm and accuracy of $\pm$ 0.5 nm for a standard 1200 gr/mm grating. The read-out of the spectrometer is a four digit wavelength counter calibrated in nanometers that displays the central wave length of light that will pass through the spectrometer for a 1200 gr/mm grating.

b) Digiscop multimate graphics program.

To record a spectrum you need to acquire and store a lot of data sets which usually

include the spectral position and the appropriate corresponding physical quantity. The data acquisition of the incoming voltage signal from the digital multimate were performed by this software. This spectral data from the spectral scan were filed as ASCII files. MicroCal Origin version 3.5 software for Windows were used to draw the graphs.

(9) Cables.

Standard BNC cables and other wires are used for electrical connection.

3.2 Experimental Procedures

3.2.1 Reflectance Measurement at Near Normal Incidence

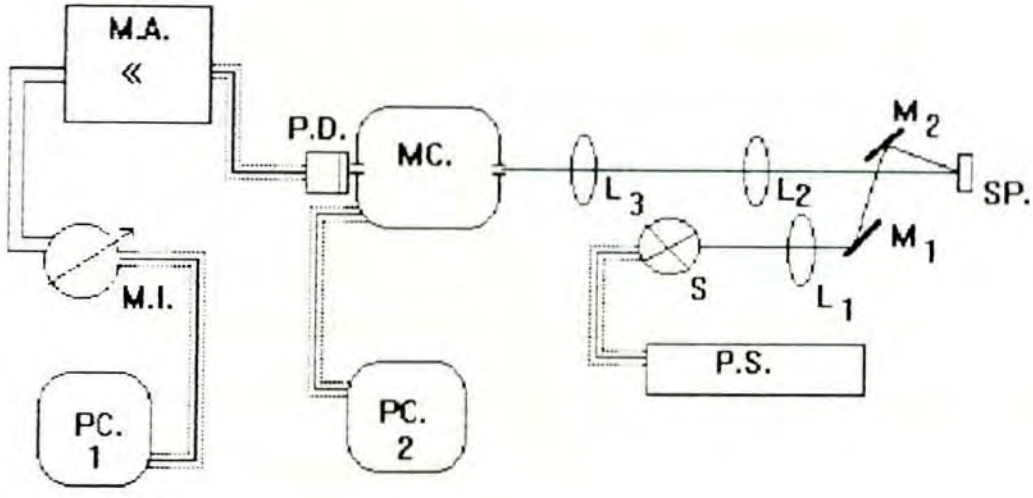

Fig. 3.1. Experimental arrangement for reflectance measurement.

M.A. : measuring amplifier, M.I. : measuring instrument (multimeter),
P.D. : photodetector, MC. : monochromator, SP. : sample, M : mirror,
P.S. : power supply, PC. : personal computer, L : lens, S : lamp.

1) A 50 mm diameter bi/convex lens of 50 mm focal length (L_1) was placed at a distance of 21cm to condense light from the halogen lamp (S).

2) A plane mirror (M_1) tilted 50^0 from the horizontal was placed at a distance of 10 cm from the condensing lens to reflect light to another plane mirror (M_2) tilted at 45^0 from the horizontal. M_2 was placed on the opposite side of an adjacent optical bench at a distance of 3.08 cm from the sample holder (SP.) to ensure near normal incidence.

3) A bi/convex lens (L_2) of 71 mm diameter with focal length 150 mm was placed at 20.9 cm from the sample to collect the light beam reflected from our samples.

4) A bi/ convex lens of 38 mm diameter (L_3) with focal length 50 mm was placed at 13.2 cm from L_2 to condense and focus the light on the entrance slit which is on the lateral side of the spectrometer (M.C.).

5) The detector (P.D.) was placed just at the exit slit on the other lateral side of the spectrometer.

6) The computers, amplifier, and power supply of the lamp were connected to the mains supply socket.

7) The output of the detector was connected to the BNC input of the current- voltage amplifier (M.A.) to amplify the incoming photocurrent. The out put of the amplifier was connected to the input of the digital multimeter (M.I.).

8) The output of the digital multimeter was connected to the first personal computer (PC_1) as shown in the figure above (Fig.3.1) which is to be loaded with the digiscop multimate graphics program software.

9) The amplifier and the digital multimeter were powered on and then checked for the connection of the computer with the multimeter. The current range was selected to be 10^{-7}A for the maximum of 2 V out put and the minimum back ground reading on the multimeter were adjusted.

10) The spectrometer was connected with the second personal computer (PC_2) which is to be loaded with the 232_SCAN.BAS program. The connection was checked by starting the computer and running the program.

11) The halogen lamp was powered on and the slit widths of both the entrance and the exit slit of the spectrometer was set to be 1 mm. The possible positions to be set for the optical components is checked by the maximum reading on the digital multimeter.

12) Finally, setting the two computers at a time the data were stored, copied on the floppy disc, and later on worked within the MicroCal Origin Window program software.

3.2.2 Transmittance Measurement at Near Normal Incidence

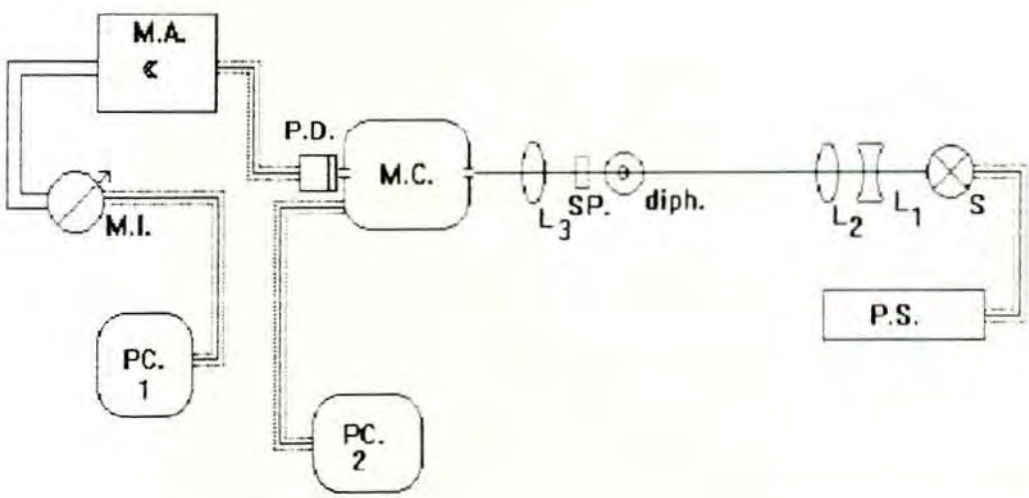

Fig. 3.2 Experimental arrangement for transmittance measurement.

M.A. : measuring amplifier, M.I. : measuring instrument (multimeter),
P.D. : photodetector, MC. : monochromator, SP. : sample,
P.S. : power supply, PC. : personal computer, L : lens, S : lamp,
diph. diphragm.

1) A 71 mm diameter bi/ concave lens (L_1) of focal length 100 mm was placed at a distance of 15 cm in front of the halogen lamp. A bi/ convex lens (L_2) of the same diameter with focal length 150 mm was placed after (L_1) altogether to make the light beam parallel.

2) A diaphragm (diph.) apertured with 60 mm diameter was placed at 41.65 mm from the second lens (L_2) to make a narrowed beam fall on our sample.

3) A sample holder (SP.) with clips was placed at 7.44 cm after the diaphragm.

4) A 38 mm diameter bi/ convex lens of 50 mm focal length (L_3) was placed 11cm from the diaphragm (diph.) to collect and focus the transmitted light beam on the entrance slit of the spectrometer.

5) The detector (P.D.) was placed just at the exit slit of the spectrometer (M.C.).

6) All the steps from (7) up to (12) taken in the reflectance measurements were repeated.

3.3 Experimental Notes

Like any other measurements both the reflectance and the transmittance measurements are measured relative to some reference. The reference sample for the reflectance measurements were an uncalibrated glass mirror while for the transmittance measurements the base substrate, corning glass were used. Its optical constant is not absolutely known. For these reasons the reflectance and the transmittance values are given in arbitrary units.

In the reflectance measurements or transmittance measurements, the spectra of the samples were taken by putting them one after another in the sample holder after the reference sample spectra is taken. In doing so, each time there will be a slight change in the angular position of the sample holder. As optical measurements are sensitive to slight change in the position of one of the optical components the reading for the maximum radiant beam which has changed in to an electrical siginal were checked by the digital multimeter each time the sample has changed.

Further improvment for the experimental set up:

a) calibrated reference mirror.

b) use of light-fiber optics to avoid readjustement after changing of samples and reference samples.

4. Reflectance and Transmittance Measurements of Thin Film a-Si : H Samples

The basic method for evaluating the optical constants of a thin film in which interference phenomena can be observed when it is exposed to light consists of referring to the reflectance (R) and transmittance (T) measurements.

The samples for investigation were deposited using plasma enhanced chemical vapour deposition (PECVD) or glow discharge (GD) deposition at radio frequency (RF) in the research centre Juelich (Germany) in the Institute for Thin Films and Ion Technique Photovoltaic (ISI - PV). Table 4.1 gives the type and thickness of the films.

The optical properties of these samples were investigated in two differernt laboratories. This was done by the same technique, but with a different experimental set up. R and T measurements of the samples in the Department of Physics of the Addis Ababa University (AAU) were carried out over an energy range of 1.24 eV < E < 3.43 eV while in the Juelich laboratory the samples were investigated over an energy range of 1.13 eV < E < 4.13 eV. The obtained results to be compared are described in the following sections.

Table 4.1 Type and thickness of samples investigated in the two laboratories: AAU and Juelich.

Sample Name	Sample Type	*Thickness* ($\cong d$) (nm)
p 1000	p doped a-Si : H	1,000
in 1000	intrinsic a-Si : H	1,000
in 100	intrinsic a-Si : H	100
n 1000	n doped a-Si : H	1,000

4.1 Reflectance Measurements

4.2.1 The p- Layer

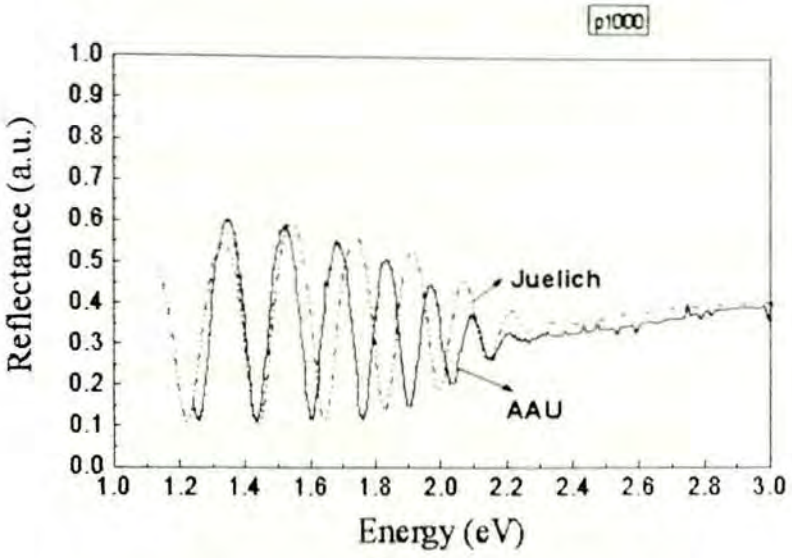

Fig. 4.1 Reflectance spectra of d ≅ 1000 nm thick p- layer of RF PECVD produced a-Si : H as measured in the two different laboratories : AAU and Juelich.

The above graph displays the reflectance spectra of an approximately 1000 nm thick p-doped a-Si : H thin film. The data is taken from the reflectance measurements done in the two different laboratories at room temperature :

AAU - Addis Ababa University Faculty of Science in the Department of Physics.

Juelich - Institute for Thin Films and Ion Technique photovoltaic (ISI - PV) Juelich, Germany.

The two spectra have a similar trend with respect to the energy range of investigation except for the different periodicity of the reflectance maxima.

The interference fringes seen in the energy region of 1.25 eV < E < 2.27 eV for the data from the AAU and in the energy region 1.22 eV < E < 2.23 eV for the data from the Juelich are due to the thickness of the film. The amplitudes of the reflectance maxima decreases from lower energies to higher energies. The decrease in amplitude is relatively large in the energy range between 1.7 eV < E < 2.1 eV for the data taken from the AAU laboratory and in the energy range of 1.7 eV < E < 2.2 eV for the data taken from the Juelich laboratory. The

decrease ranges from 4 % - 18 % of the maximum value for the data from AAU and from 4 % -22 % for the data from Juelich. The half widths of the interference fringes are also smaller in this energy range. No interference fringes are seen in the energy ranges which are above 2.27 eV for the measurements done in both laboratories. The spectral positions of the reflectance maxima with their corresponding errors of measurement are given in Table 4.2.

Table 4.2 Reflectance maxima values for an approximately 1000 nm thickness p- layer of a- Si : H with thier corresponding accuracy of measurement as measured in the two different laboratories : AAU and Juelich.

	Reflectance maxima (eV)	
Maxima no.	AAU	Juelich
1	1.346 +/- 0.13	1.334 +/- 0.14
2	1.522 +/- 0.10	1.536 +\- 0.12
3	1.683 +/- 0.11	1.747 +/- 0.11
4	1.830 +/- 0.08	1.914 +/- 0.09
5	1.972 +/- 0.07	2.072 +/- 0.08
6	2.090 +/- 0.09	2.206 +/- 0.09

4.1.2 The Thick i- Layer

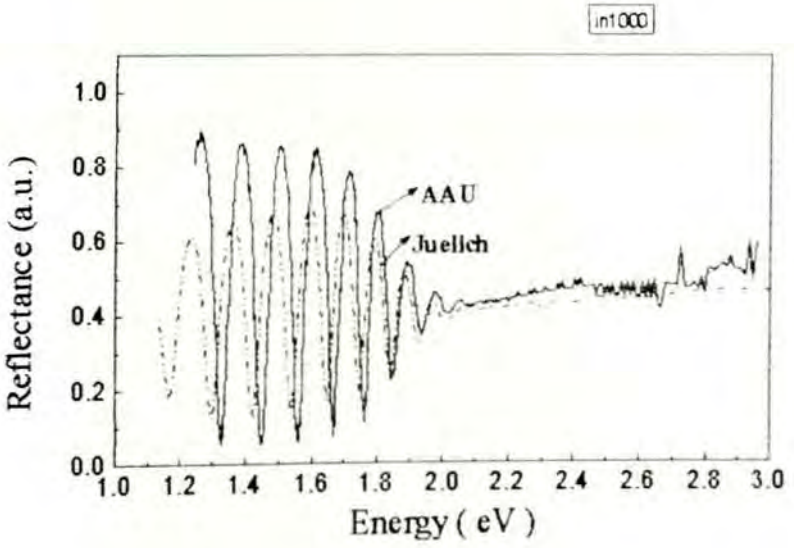

Fig. 4.2 Reflectance spectra of d ≅ 1000 nm thick i- layer of RF PECVD produced a-Si : H as measured in the two different laboratories : AAU and Juelich.

In Fig. 4.2 the reflectance spectra of approximately 1000 nm thick intrinsic layer of a-Si : H thin film is displayed. The data is taken from the reflectance measurement done in the two different laboratories at room temperature : AAU and Juelich

The two spectra have a similar trend with respect to each energy ranges of investigation except for the different periodicity of the reflectance maxima.

The interference fringes are seen in the energy region of 1.24 eV < E < 2.01 eV for the data from the AAU laboratory. For the data from the Juelich laboratory the interference fringes are seen in the energy region of 1.16 eV < E < 2.01 eV. These interference fringes are due to the thickness of the film. The amplitude of the reflectance maxima decreases from lower energies to higher energies. The decrease in amplitude is relatively large in the energy range of 1.7 eV < E < 1.98 eV for the data from the AAU and in the energy range of 1.7 eV < E < 1.96 eV for the data from Juelich. The decrease ranges from 7 % - 30 % of the maximum value for the data from AAU and from 3 % - 19 % of the maximum value for the data fromJuelich. The half widths of the interference fringes are broader for lower energies as compared to higher energies. No interference fringes are seen in the energy range which is above 2.01 eV for the measurements done in both laboratories. The spectral positions of the reflectance maxima with their corresponding errors of measurement are given in Table 4.3.

Table 4.3 Reflectance maxima values for an approximately 1000 nm thickness i - layer of a- Si : H with their corresponding accuracy of measurement as measured in the two different laboratories : AAU and Juelich.

	Reflectance maxima (eV)	
Maxima no.	AAU	Juelich
0	1.259 +/- 0.10	1.232 +/- 0.10
1	1.388 +/- 0.12	1.357 +/- 0.09
2	1.504 +/- 0.09	1.477 +/- 0.09
3	1.610 +/- 0.09	1.593 +/- 0.07
4	1.712 +/- 0.06	1.700 +/-0.06
5	1.805 +/- 0.06	1.788 +/- 0.05
6	1.889 +/- 0.04	1.876 +/- 0.06
7	1.981 +/- 0.07	1.964 +/- 0.06

4.1.3 The Thin i- Layer

In figure below (Fig. 4.3) the reflectance spectra of an approximately 100 nm thickness intrinsic layer of a-Si : H thin film is displayed. The data is taken from the reflectance measurements done in the two laboratories.

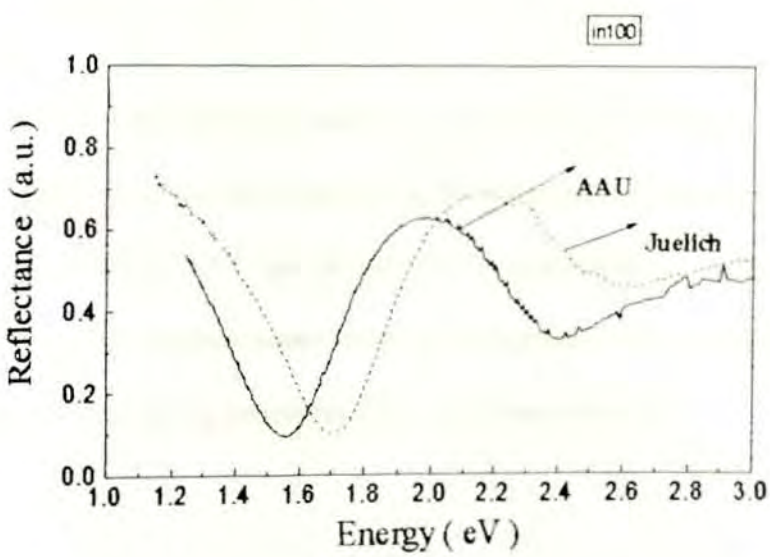

Fig. 4.3 Reflectance spectra of d ≅ 100 nm thick i - layer of RF PECVD produced a-Si : H as measured in the two different laboratories : AAU and Juelich.

The two spectra have a similar characteristics with respect to the energy range of investigation except for the mismatch of the reflectance maxima energy positions. The reflectance maximum for the data from the AAU laboratory shifts by 0.17 eV to lower energy with respect to the reflectance maximum measured in Juelich.

Unlike the thicker i- layer here we have only one reflectance maximum. The width of the interference fringe is also the broadest measured than all of the other samples. It is 0.63 eV for the data from the AAU laboratory and 0.88 eV for that from Juelich laboratory. The spectral positions of the reflectance maxima with their corresponding accuracy of measurement are given in Table 4.4 for the measurement done in both laboratories.

Table 4.4 Reflectance maxima values for an approximately 100 nm thickness i- layer of a- Si : H with their corresponding accuracy of measurement as measured in the two different laboratories : AAU and Juelich

	Reflectance maxima (eV)	
Maximum no.	AAU	Juelich
1	1.989 +/- 0.63	2.156 +/- 0.88

4.1.4 The n - Layer

In Fig. 4.4 the reflectance spectra of an approximately 1000 nm thickness n- layer of a-Si : H thin film is displayed. The data is taken from the reflectance measurements done in the two different laboratories: AAU and Juelich. The measurements are done at room temperature. The two spectra have a similar trend with respect to each energy ranges of investigation except for the different periodicity of the reflectance maxima.

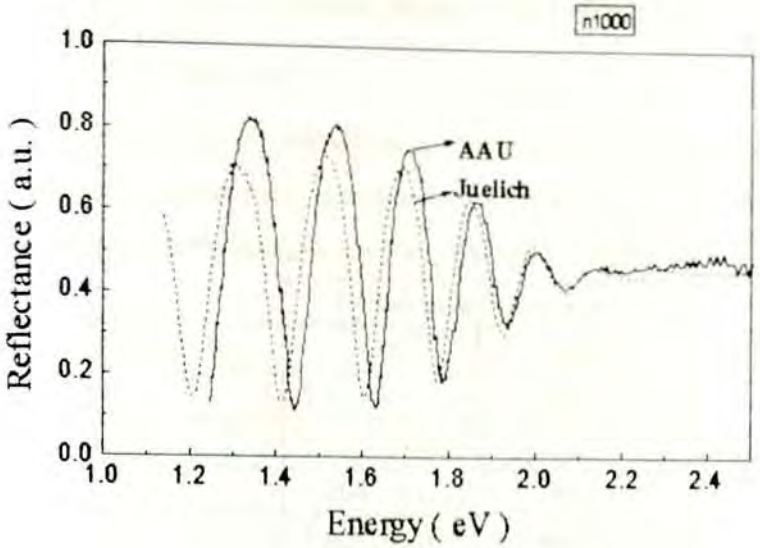

Fig. 4.4 Reflectance spectra of d ≅ 1000 nm thick n- layer of RF PECVD produced a-Si : H as measured in the two different laboratories : AAU and Juelich.

The interference fringes are seen in the energy region of 1.24 eV < E < 2.06 eV for the data from the AAU laboratory. For the data from the Juelich laboratory the maxima of interference fringes are seen in the energy region of 1.20 eV < E < 2.06 eV. These interference fringes are due to the thickness of the film. The amplitude of the reflectance maxima decreases from lower energies to higher energies. The decrease in amplitude is relatively more pronounced in the energy range of 1.70 eV < E < 1.99 eV for the data from the AAU laboratory and in the energy range of 1.69 eV < E < 1.99 eV for the data from Juelich. The decrease ranges from 16 % - 29 % of the maximum value for the data taken from the AAU laboratory and from 15 % - 30 % of the maximum value for the data from that of the Juelich laboratory. The half widths of the interference fringes are broader for lower energies as compared to that at higher energies. No interference fringes are seen in the energy range which is above 2.06 eV for the measurements done in both laboratories.

The half widths of the interference fringes of this layer are broader than that of the thicker intrinsic layer and the p- layer. This is true for the data taken from both laboratories.

The spectral positions of the reflectance maxima with their corresponding errors of measurements are given in Table 4.5.

Table 4.5 Reflectance maxima values for an approximately 1000 nm thickness n- layer of a- Si : H with thier corresponding accuracy of measurements as measured in the two different laboratories : AAU and Juelich.

	Reflectance maxima (eV)	
Maxima no.	AAU	Juelich
0	1.334 +/- 0.16	1.294 +/- 0.18
1	1.536 +/- 0.15	1.512 +/- 0.13
2	1.708 +/- 0.12	1.692 +/- 0.12
3	1.860 +/- 0.09	1.849 +/-0.09
4	1.997 +/- 0.13	1.995 +/-0.14

4.2 Transmittance Measurements

4.2.1 The p- Layer

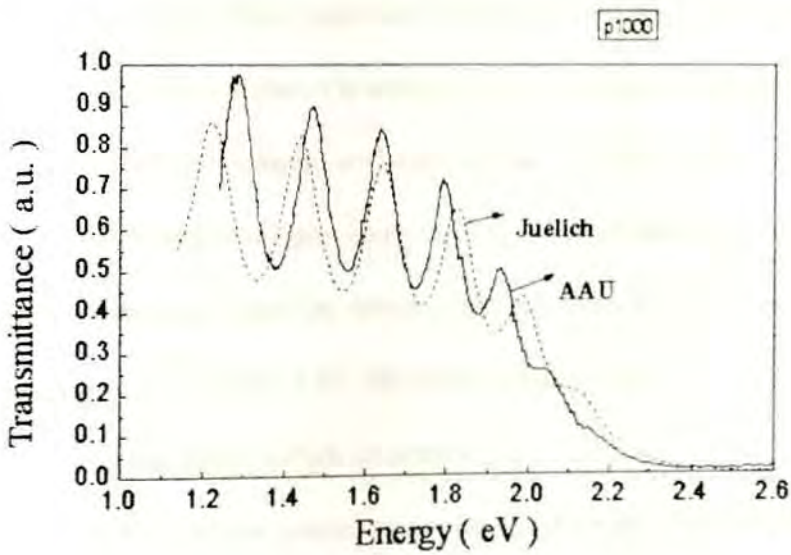

Fig. 4.5 Transmittance spectra of d ≅ 1000 nm thick p - layer of RF PECVD produced a-Si : H as measured in the two different laboratories : AAU and Juelich.

The above graph (Fig. 4.5) shows the transmittance spectra of an approximately 1000 nm thickness p- layer of a-Si : H thin film. The data is taken from the measurement done in the two laboratories at room temperature. Similar to the reflectance spectra, the transmittance spectra from the two laboratories, have a similar characteristics except for the different periodicity of the transmittance maxima.

Interference fringes are seen in the energy range of 1.24 eV < E < 2.02 eV for the transmittance measurement done in the AAU laboratory. For the data from Juelich the interference fringes are seen in the energy range of 1.13 eV < E < 2.07 eV. These interference fringes are again due to the thickness of the films. The amplitude of the transmittance maxima decreases from lower energies to higher energies which is similar to the behaviour of the reflectance maxima. The decrease in amplitude is relatively larger in the energy range of 1.63 eV < E < 1.93 eV for the data from AAU and in the energy range of 1.64 eV < E < 1.98 eV for that from Juelich. The decrease in amplitude ranges from 7 % to 47 % of the maximum transmittance amplitude for the data from the AAU laboratory while it is from 4 % to 43 % of the maximum transmittance for the data taken from that of the Juelich laboratory. No interference fringes are seen on the average above 2.07 eV and no transmittance is seen at higher energies above 2.4 eV. The transmittance, at this energy limit, above which no transmittance could be detected by the detector has a non-zero value (E ~ 0.01 eV) for the data from the AAU laboratory while it is (E ~ 0.004 eV) for the measurement done in that of the Juelich laboratory.

The spectral positions of the transmittance maxima with their corresponding errors of measurment are given in Table 4.6.

Table 4.6 Transmittance maxima values for an approximately 1000 nm thickness p- layer of a- Si : H with their corresponding accuracy of measurement as measured in the two different laboratories : AAU and Juelich.

	Transmittance maxima (eV)	
Maxima no.	AAU	Juelich
1	1.285 +/- 0.07	1.220 +/- 0.08
2	1.470 +/- 0.06	1.438 +/- 0.07
3	1.636 +/- 0.06	1.641 +/- 0.07
4	1.792 +/- 0.05	1.822 +/- 0.07
5	1.933 +/- 0.08	1.985 +/- 0.09

4.2.2 The Thick i- Layer

The figure below (Fig. 4.6.) shows the transmittance spectra of approximately 1000 nm thick i- layer of a-Si : H thin film. Both data are taken from the measurement done in the two laboratories at room temperature.

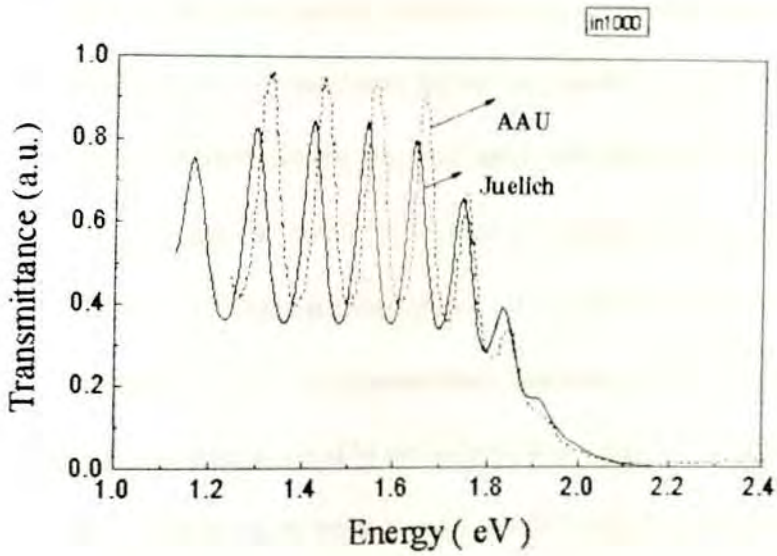

Fig.4.6 Transmittance spectra of d ≅ 1000 nm thick i- layer of RF PECVD produced a-Si : H as measured in the two different laboratories : AAU and Juelich

The two transmittance spectra have a similar trend except for the different periodicity of the transmittance maxima. As compared to the transmittance maxima of the other samples investigated the mismatch is relatively very small.

Interference fringes are seen in the energy range of 1.13 eV < E < 1.90 eV for the transmittance measurement done in the Juelich laboratory. For the data taken from that of the AAU the interference fringes are seen in the energy range of 1.26 eV < E < 1.90 eV. Different from that of the data from the Juelich laboratory one of the transmittance maxima is absent in the transmittance spectra of the data from that of the AAU due to the near - infrared limitation of the experimental set-up. The amplitude of the transmittance maxima decreases from lower energies to higher energies which is of the same beaviour as observed for the reflectance maxima. The decrease in amplitude is relatively large in the energy range of 1.66 eV < E < 1.84 eV for the data from the AAU laboratory and in the energy range of 1.64 eV < E < 1.83 eV for that from Juelich. These decrease in amplitude ranges from 8 % to 27 % of the maximum transmittance amplitude for the data taken from AAU and from 5 % to 14 % of the maximum transmittance for the data taken from Juelich laboratory. The half width of the interference fringes are small ($\Delta\nu \sim 0.04$ eV) unlike the other samples and are nearly equal. No interference fringes are seen above 1.90 eV and no transmittance is seen at the higher energies above 2.15 eV. The transmittance amplitude at this energy limit, above which no transmittance could be detected by the detector has a non- zero value ($E \sim 0.01$ eV) for the data from the AAU laboratory while it is ($E \sim 0.001$ eV) for the measurement done in that of Juelich.

The spectral positions of the transmittance maxima with their corresponding errors of measurement are given in Table 4.7.

Table 4.7 Transmittance maxima values for an approximately 1000 nm thickness i- layer of a- Si : H with their corresponding accuracy of measurements as measured in the two different laboratories: AAU and Juelich. * - Transmittance spectra which is absent due to the investigation range.

	Transmittance maxima (eV)	
Maxima no.	AAU	Juelich
0	*	1.165 +/- 0.05
1	1.325 +/- 0.04	1.294 +/- 0.04
2	1.447 +/- 0.03	1.422 +/- 0.04
3	1.555 +/- 0.04	1.536 +/- 0.04
4	1.664 +/- 0.03	1.648 +/- 0.03
5	1.755 +/- 0.03	1.747 +/- 0.04

4.2.3 The Thin i- Layer

In figure below (Fig. 4.7) the transmittance spectra of approximately 100 nm thick intrinsic layer of a-Si : H thin film is displayed. The data is taken from measurements done in the two laboratories at room temperature.

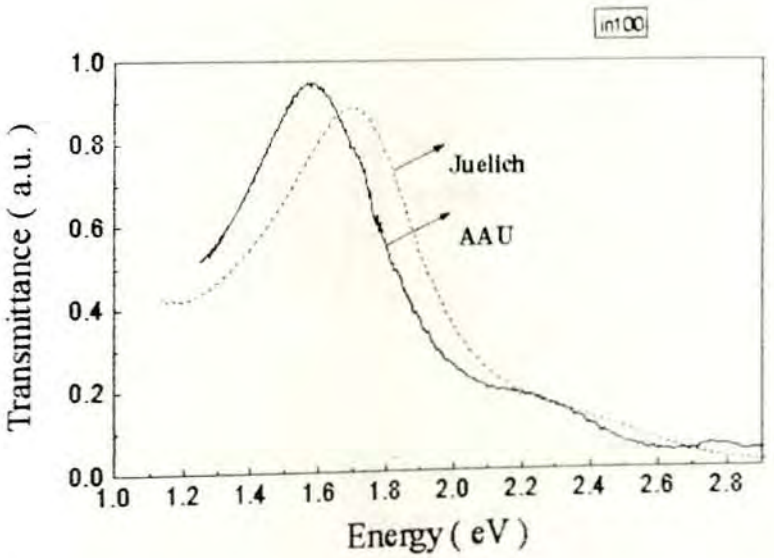

Fig. 4.7 Transmittance spectra of d ≅ 100 nm thick i- layer of RF PECVD produced a-Si : H as measured in the two different laboratories : AAU and Juelich.

The two spectra have a similar trend except for the relatively large mismatch (~ 0.11eV)

of the maximum energy position and a non-zero amplitude (~ 0.04 eV) at the higher energy limit above which no transmittance is seen in this investigation. Differing from the other samples, a non-zero amplitude value (~ 0.01 eV) is also observed for the data obtained from the Juelich laboratory.

For this sample, which is approximately ten times thinner than the others, only one maximum is obtained. The spectral position of this transmittance maximum is given in Table 4.8 with its uncertainity of measurement.

Table 4.8 Transmittance maximum value for approximately 100 nm thick i- layer of a- Si : H with their corresponding accuracy of measurement as measured in the two different laboratories: AAU and Juelich.

	Transmittance maximum (eV)	
Maximum no.	AAU	Juelich
1	1.564 +/- 0.39	1.692 +/- 0.31

4.2.4 The n- Layer

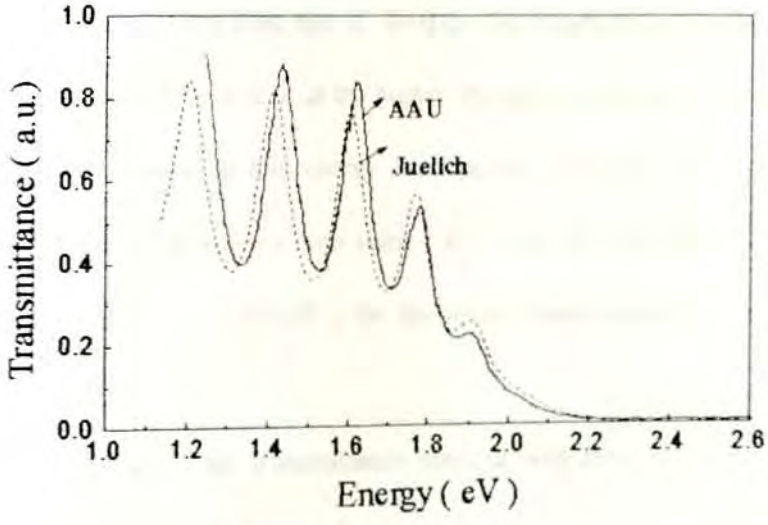

Fig. 4.8 Transmittance spectra of d ≅ 1000 nm thick n- layer of RF PECVD produced a-Si : H as measured in the two different laboratories : AAU and Juelich.

The above figure (Fig. 4.8) shows the transmittance spectra of an approximately 1000 nm thickness n- layer of a-Si : H thin film. The data is taken from the measurements done in the two laboratories at room temperature. The transmittance spectra have a similar trend except for the different periodicity of the transmittance maxima.

Interference fringes are seen in the energy range of 1.24 eV < E < 1.85 eV for the transmittance measurement done in the AAU laboratory. For the data from Juelich they are seen in the energy range of 1.13 eV < E < 1.85 eV. Different from that of the data taken from the Juelich laboratory one of the transmittance maxima is absent in the transmittance spectra for the data taken from AAU. The amplitude of the transmittance decreases from lower energies to higher energies which is the similar to that for the reflectance maxima. The decrease in amplitude is relatively large in the energy range of 1.61 eV < E < 1.77 eV for the data from the AAU laboratory and in the energy range of 1.60 eV < E < 1.77 eV for that from Juelich. These decrease in amplitude ranges from 5 % to 35 % of the maximum transmittance amplitude for the data taken from the AAU and from 5 % to 25 % of the maximum transmittance for the data taken from that of Juelich. No interference fringes are seen above 1.85 eV and no transmittance is seen at the higher energies on the avearage above 2.25 eV. The transmittance amplitude, at this energy limit above which no transmittance could be detected by the detector has a non - zero value (E ~ 0.01 eV) for the data from the AAU laboratory while it is (E ~ 0.001eV) for the measurement done in that of the Juelich laboratory.

The spectral positions of the transmittance maxima with their corresponding errors of measurement are given below in Table 4.9.

Table 4.9 Transmittance maxima values for an approximately 1000 nm thickness n- layer of a- Si : H with thier corresponding accuracy of measurement as measured in the two different laboratories: AAU and Juelich.

	Transmittance maxima (eV)	
Maxima no.	AAU	Juelich
0	*	1.201 +/- 0.07
1	1.432 +/-0.06	1.412 +/- 0.07
2	1.614 +/- 0.06	1.600 +/- 0.06
3	1.777 +/- 0.07	1.771+/- 0.07

4.3 Absorption Coefficient of p- , i- , and n- Layers of a-Si : H

The absorption coefficient (α) is calculated for all of the samples using Hishikawa's relation (given in section two) from the R and T data obtained from both laboratories. The absorption spectra for the investigated samples are shown with the abscissa in the logarithmic scale (to compare the orders of magnitude) of the absorption coefficient in the units of cm^{-1} and the ordinate axis in a linear scale of energy in the units of eV.

The energy ranges shown in the spectra are only what considered as medium and strongly absorbing regions. These are the regions where the curves in their absorption spectra are smooth. There is also an absorption even in the energy ranges below the E_g^{opt} which is directly related to the localazed energy states or traps in the mobility gap [2].

4.3.1 The p- Layer

The absorption spectra of the p- layer of a-Si : H is shown in the figure (Fig. 4.9) below. The data is taken from the R and T measurements done in the two laboratories at room temperature.

The two absorption spectra have a similar trend in the energy range $1.8\ eV < E < 2.4\ eV$. Nevertheless, the absorption spectrum from R and T data obtained from the AAU laboratory

is slightly at higher values with respect to that from Juelich. The residual non- linear parts in the spectra which are seen below 2.05 eV are relatively medium absorbing regions.

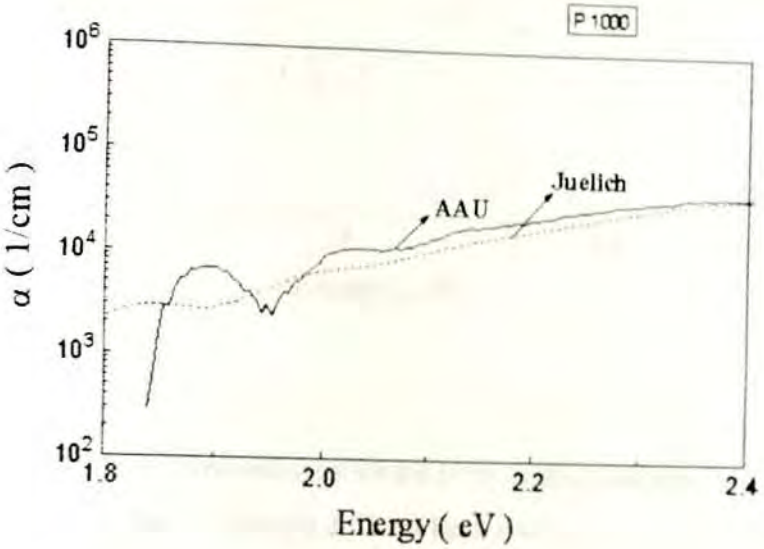

Fig. 4.9 Absorption coefficient for the 1000 nm thick p- layer of a-Si : H as measured in the two different laboratories.

The amplitudes of the maxima of the interference structure seen in this region are relatively higher for the data from the AAU laboratory than that from the Juelich laboratory.

4.3.2 The Thick i- Layer

The absorption spectra of the thicker i- layer of a-Si : H is shown in the figure (Fig. 4.10) below. The data is taken from the R and T measurments done in the two laboratories at room temperature. The two absorption spectra have a similar trend in the energy range of 1.6 eV < E < 2.15 eV and they are even equal in the energy range of (1.90 eV < E < 2.15 eV).The amplitude of the maximum of the residual interference structure in the relatively medium absorbing regions, below 1.90 eV are relatively higher for the data from the AAU than that from Juelich.

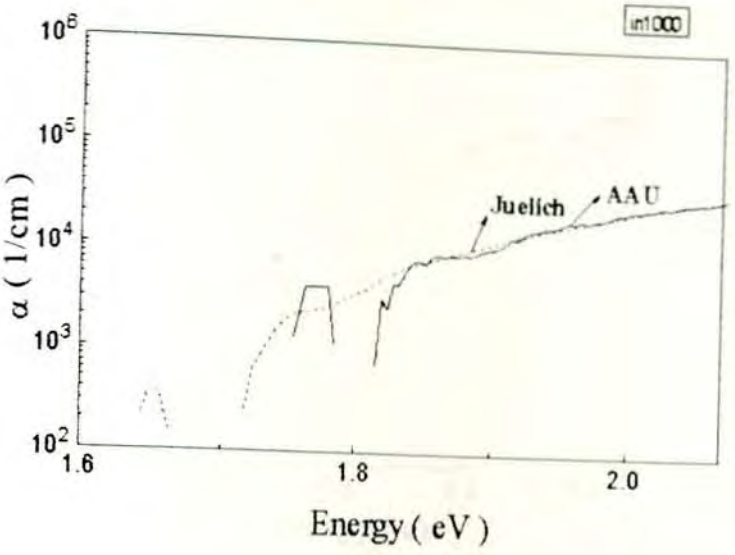

Fig. 4.10 Absorption coefficient for the 1000 nm thick intrinsic layer of a-Si : H as measured in the two different laboratories.

4.3.3 The Thin i- Layer

The absorption spectra of the thinner i- layer of a-Si : H is displayed in the figure (Fig. 4.11) below. The data is taken from the R and T measurements done in the two laboratories. Both data are taken at room temperature. The two absorption spectra have a similar trend in the energy range 1.6 eV < E < 2.60 eV except that the spectrum obtained from the R and T data from the AAU laboratory is slightly higher with respect to that from the Juelich laboratory. The spacing between the two spectra is larger as compared to other samples. Different from the thicker layers no interference structures are seen on the spectra.

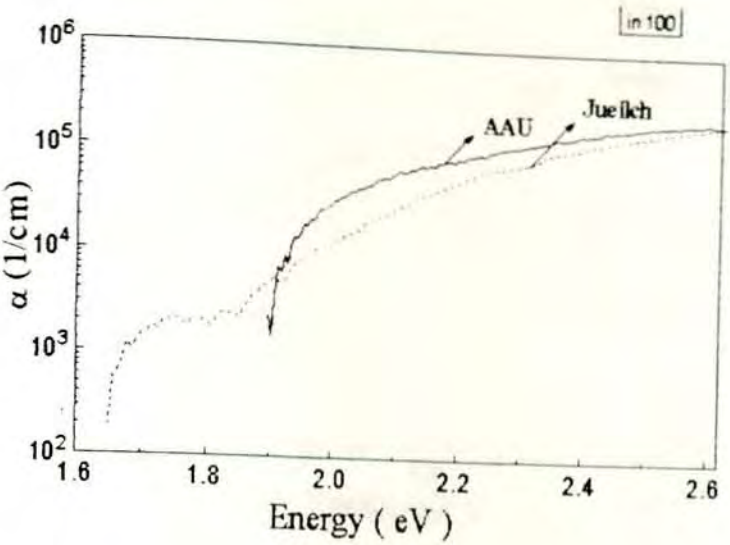

Fig. 4.11 Absorption coefficient for the 100 nm thick intrinsic layer of a-Si : H as measured in the two different laboratories.

4.3.4 The n- Layer

The graph below (Fig.4.12) displays the absorption spectra of the n- layer for the R and T measurements done in the two laboratories at room temperature. The two absorption spectra have a similar character in the energy range of 1.84 eV < E < 2.25 eV. However, the absorption spectrum from R and T data obtained from the AAU laboratory is slightly higher with respect to that from Juelich.

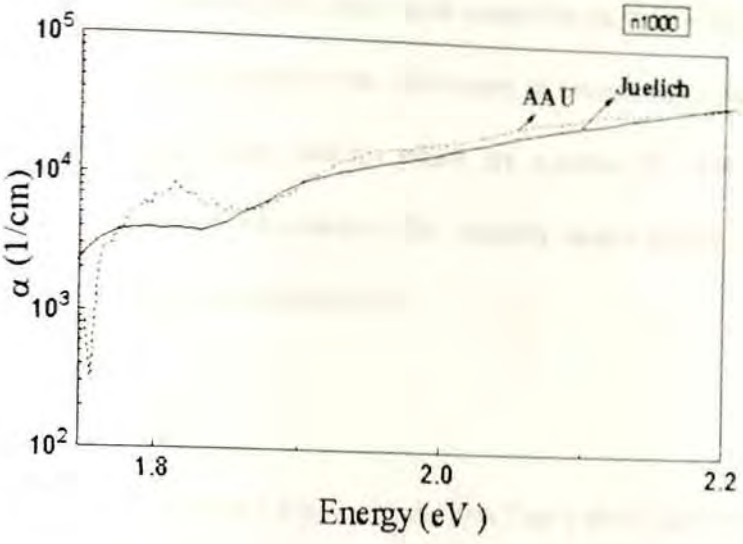

Fig.4.12 Absorption coefficient for the 1000 nm thick n- layer of a-Si : H as measured in the two different laboratories.

The amplitude of the maximum of the interference structure seen in the spectra below 1.85 eV is relatively higher for the data from the AAU than that from Juelich.

4.4 Optical Band Gaps of p-, i-, and n- Layers

Out of the various ways of presenting the optical gaps, that of Tauc's, which is a more conventional approch and where the optical band gap is obtained by extrapolating the plot of $(\alpha nE)^{1/2}$ versus energy to zero ordinate [18] were used. Of course, extrapolation of the plot of $(\alpha E)^{1/2}$ which is probably most often used to evaluate the optical gap from the R and T data had also been used for the thin i- layer optical gap determination for the reason having no interference fringes pattern seen from which the refractive index, n can be calculated.

The refractive index for all samples except for the thin i- layer is calculated from both R and T data obtained in the two laboratories. The corresponding Tauc's plot from which the optical gaps are determined is shown for all layers for comparison. Tauc's plot from R data

and T data are shown separately for each layers except for the thin i- layer. In determining the refractive index at energies where the reflectance or transmittance maxima are seen we had used the interference fringe maxima which are common for both energy ranges of investigation used in the two laboratories. The linearity ranges shown in the plots are the ones which are common in both laboratories.

4.4.1 The p- Layer

As it is seen in figure below (Fig. 4.13) the two Tauc's plots have a similar trend. As it is only a transformation of the absorption spectra, the plot from the data obtained from the AAU laboratory is slightly higher (giving rise to relatively lower optical bandgap value) than that from the Juelich laboratory. Interference structure with larger amplitudes compared to their absorption spectra are also seen on the two plots in the relatively medium absorbing regions.

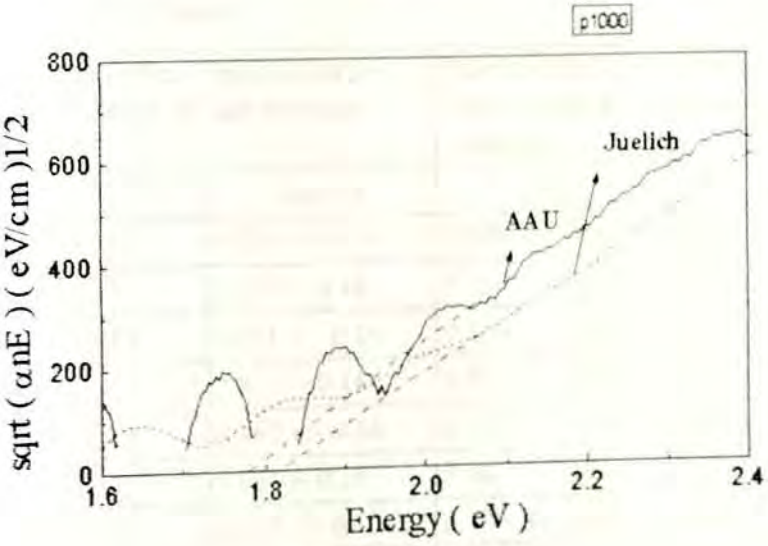

Fig.4.13 Tauc's plot for the p- layer using refractive index, n from the room temperature reflectance data obtained in the two laboratories.

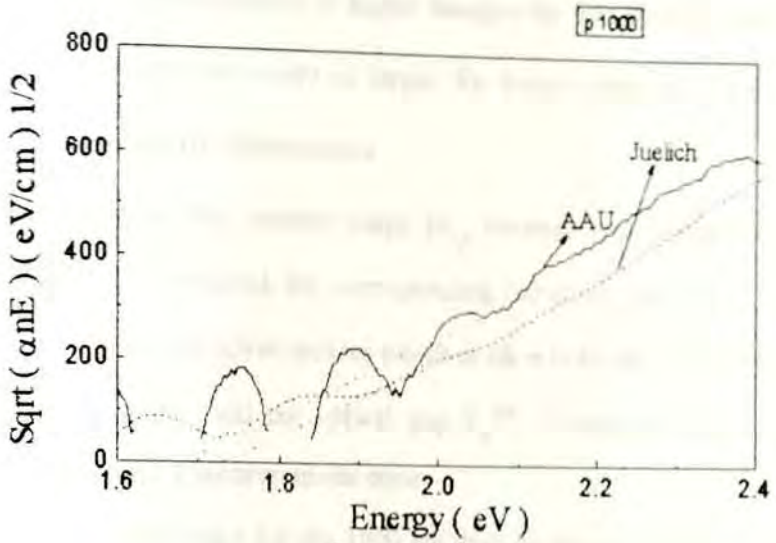

Fig.4.14 Tauc's plot for the p- layer using refractive index, n from room temperature transmittance data obtained in the two laboratories.

Table 4.10 Free spectral range $\delta\nu_{ij}$, refractive indices n_{ij}, average refractive index n_{av}, optical gap E_g^{opt}, with their corresponding errors of measurements for the a-Si : H p- layer.

	Reflectance free spectral ranges, optical gap in eV and refractive indices.		Transmittance free spectral ranges, optical gap in eV and refractive indices.	
	AAU	Juelich	AAU	Juelich
$\delta\nu_{21}$	0.176 +/- 0.16	0.201 +/- 0.18	0.184 +/- 0.09	0.218 +/- 0.11
n_{21}	3.50 +/- 0.16	3.07 +/- 0.18	3.35 +/- 0.09	2.84 +/- 0.11
$\delta\nu_{32}$	0.160 +/- 0.15	0.211 +/- 0.16	0.166 +/- 0.08	0.203 +/- 0.10
n_{32}	3.86 +/- 0.15	2.93 +/- 0.16	3.71 +/- 0.08	3.05 +/- 0.10
$\delta\nu_{43}$	0.146 +/- 0.14	0.167 +/- 0.14	0.155 +/- 0.08	0.180 +/- 0.10
n_{43}	4.22 +/- 0.14	3.69 +/- 0.14	3.98 +/- 0.08	3.42 +/- 0.10
$\delta\nu_{54}$	0.141 +/- 0.11	0.157 +/- 0.12	0.140 +/- 0.09	0.162 +/- 0.11
n_{54}	4.36 +/- 0.11	3.92 +/- 0.12	4.40 +/- 0.09	3.80 +/- 0.11
$\delta\nu_{65}$	0.118 +/- 0.11	0.133 +/- 0.12	_	_
n_{65}	5.22 +/- 0.11	4.63 +/- 0.12	_	_
n_{av}	4.23 +/- 0.06	3.65 +/- 0.06	3.86 +/- 0.04	3.28 +/- 0.05
E_g^{opt}	1.79 +/- 0.44 (2.06 eV-2.32 eV)	1.82 +/- 0.40 (2.06 eV-2.32eV)	1.78 +/- 0.44 (2.06 eV-2.32 eV)	1.82 +/- 0.39 (2.08 eV-2.32 eV)

As we move from lower energies to higher energies the free spectral range decreases. In contrast to this the refractive index is larger for higher energies. This is true for the measurements done in the two laboratories.

Table 4.10 gives the free spectral range $\delta\nu_{ij}$, between two successive reflectance or transmittance maxima considered, the corresponding refractive indices n_{ij}, the calculated average value n_{av}, of the refractive indices which is taken to be the refractive index of the p-layer of a-Si : H sample, and the optical gap E_g^{opt}, determined in the stated range of extrapolation from R and T measurements done.

In Fig. 4.14 the Tauc's plot for the 1000 nm thick p- layer is displayed. The refractive index used is the one obtained from transmittance data at room temperature. The plots from the data obtained in the two laboratories have a similar trend except that plot from the R and T data obtained from the AAU laboratory is slightly higher than the plot from R and T data obtained from the Juelich laboratory.

4.4.2 The Thick i- Layer

As it is seen in Fig. 4.15 the two Tauc's plots for the 1000 nm thick i- layer have a similar trend and they are even equal (different from the other samples) except for the extension of their linearity range. The refractive index used is the one obtained from room temperature reflectance measurement. The optical gap determined from the two plots are also equal (1.70 eV)

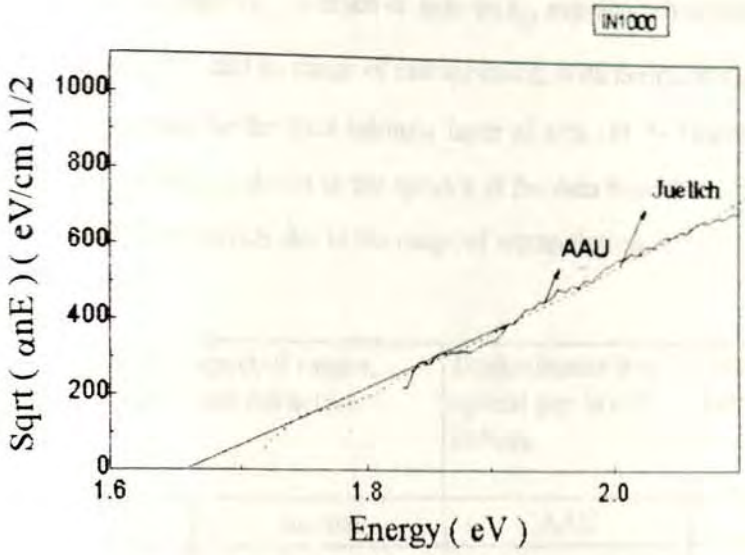

Fig. 4.15 Tauc's plot for the 1000 nm thick i- layer using refractive index from room temperature reflectance data obtained in the two laboratories.

Table 4.11 gives the free spectral range between two successive reflectance or transmittance maxima, the corresponding refractive indices calculated, the average value of the refractive indices which is taken to be the refractive index of the i- layer of a-Si : H, and the optical gap determined in the stated range of extrapolation from R and T measurements in the two laboratories.

Table 4.11 Free spectral range $\delta\nu_{ij}$, refractive indices n_{ij}, average refractive index n_{av}, optical gap E_g^{opt}, and its range of extrapolation, with their corresponding errors of measurements for the thick intrinsic layer of a-Si : H. *- Transmittance maximium which is absent in the spectra of the data from the AAU with respect to that from the Juelich due to the range of extrapolation.

	Reflectance free spectral ranges, optical gap in eV and refractive indices		Transmittance free spectral ranges, optical gap in eV and refractive indices.	
Items	AAU	Juelich	AAU	Juelich
$\delta\nu_{10}$	0.129 +\- 0.16	0.125 +/- 0.13	*	0.128 +/-
n_{10}	4.80 +/- 0.16	4.96 +/- 0.13	_	_
$\delta\nu_{21}$	0116 +/- 0.15	0.12 +/- 0.13	0.122 +/- 0.05	0.128 +/- 0.06
n_{21}	5.34 +/- 0.15	5.16 +/- 0.13	5.08 +/- 0.05	4.81 +/- 0.06
$\delta\nu_{32}$	0.106 +/- 0.13	0.116 +/- 0.11	0.108 +/- 0.05	0.113 +/- 0.06
n_{32}	5.84 +/- 0.13	5.34 +/- 0.11	5.74 +/ 0.05	5.47 +/- 0.06
$\delta\nu_{43}$	0.102 +/- 0.11	0.107 +/- 0.09	0.109 +/- 0.05	0.112 +/- 0.05
n_{43}	6.07 +/- 0.11	5.79 +/- 0.09	5.68 +/- 0.05	5.53 +/- 0.05
$\delta\nu_{54}$	0.093 +/- 0.08	0.088 +/- 0.08	0.091 +/- 0.04	0.099 +/- 0.05
n_{54}	6.66 +/- 0.08	7.04 +/- 0.08	6.81 +/- 0.04	6.26 +/- 0.05
$\delta\nu_{65}$	0.084 +/-0.07	0.088 +/- 0.08	_	_
n_{65}	7.38 +/- 0.07	7.04 +/- 0.08	_	_
$\delta\nu_{76}$	0.092 +/- 0.08	0.088 +/- 0.08	_	_
n_{76}	6.73 +/- 0.08	6.98 +/- 0.08	_	_
n_{av}	6.11 +/- 0.04	6.04 +/- 0.04	5.83 +/- 0.02	5.52 +/- 0.03
E_g^{opt}	1.70 +/- 0.57 (1.89 eV-2.07 eV)	1.70 +/- 0.57 (1.88 eV- 2.07 eV)	1.70 +/- 0.56 (1.89 eV-2.07 eV)	1.69 +/- 0.28 (1.88 eV-2.07eV

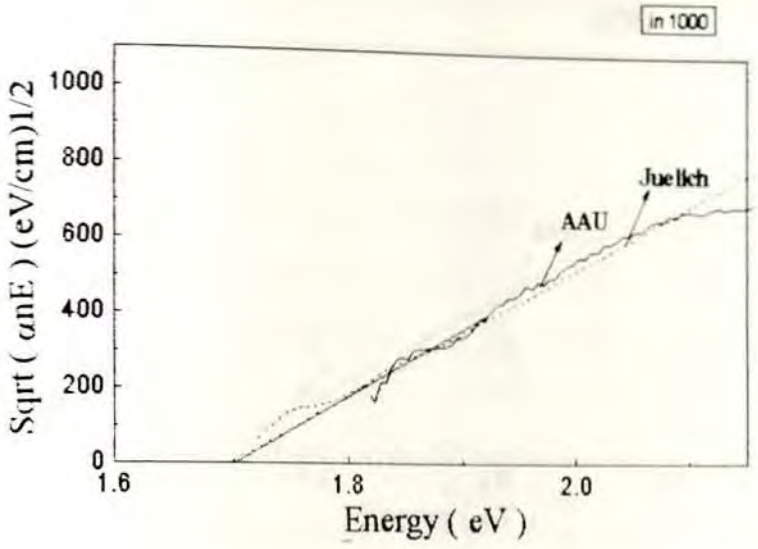

Fig.4.16 Tauc's plot for the thick i- layer using refractive index from room temperature transmittance data obtained in the two laboratories.

In Fig. 4.16 the Tauc's plot by including the refractive index determined from the transmittance spectra of the 1000 nm thick i- layer is displayed. The two plots have a similar trend and are equal except for the extension of their linearity range. The optical gap determined from the two data are equal with in the value 0.01 eV.

4.4.3 The n- Layer

In Fig. 4.17 Tauc's plots for the n- layer, to determine the optical gap from the extrapolaton of $(\alpha nE)^{1/2}$ versus E using the refractive index from the room temperature reflectance data obtained in the two laboratories are displayed. The two plots have a similar trend except for the extension of their linearity range. For the data from the AAU laboratory the linearity range extends from 1.97 eV to 2.23 eV while for the data from that of the Juelich laboratory it extends from 1.97 eV to 2.33 eV.

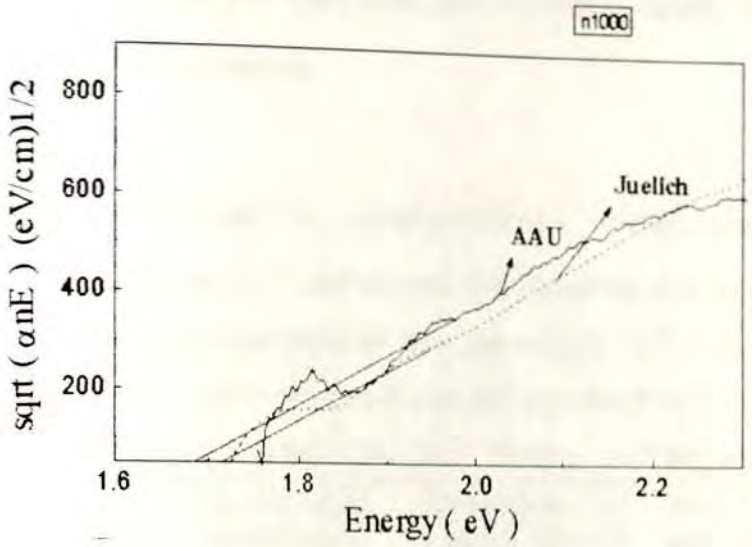

Fig. 4.17 Tauc's plot for the n- layer using refractive index from the room temperature reflectance data obtained from the two laboratories.

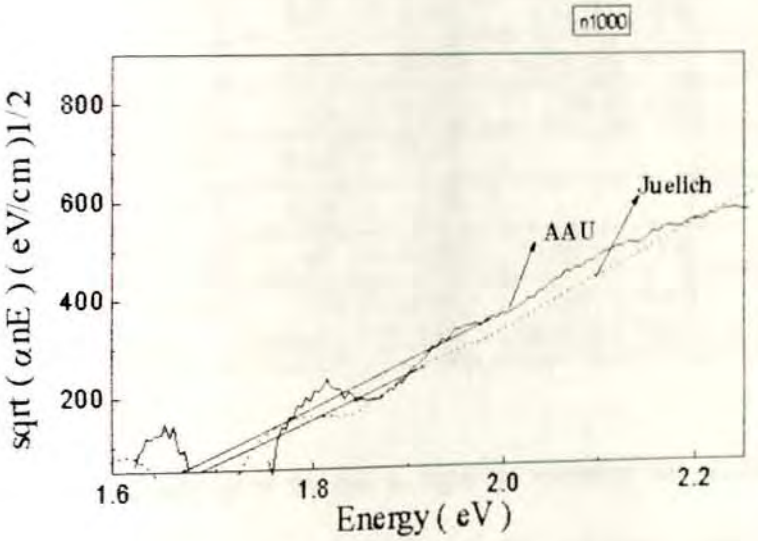

Fig. 4.18 Tauc's plot for the n- layer using refractive index from room temperature transmittance data obtained in the two laboratories.

Table 4.12 gives the free spectral range between two successive reflectance or transmittance maxima, the corresponding refractive indices calculated, the average value of the refractive indices which is taken to be the refractive index of the 1000 nm thick n- layer

of a-Si : H, and the optical gap determined in the stated range of extrapolation from R and T measurements done in both laboratories.

Table 4.12 Free spectral range $\delta\nu_{ij}$, refractive indices n_{ij}, average refractive index n_{av}, optical gap E_g^{opt}, and its range of extrapolation, with their corresponding errors of measurement for the n- layer of a-Si : H. *- Transmittance maximium which is absent in the spectra of the data from the AAU with respect to that from the Juelich due to the range of extrapolation.

	Reflectance free optical gap in eV and refractive indices. spectral ranges,		Transmittance free optical gap in eV and refractive indices. spectral ranges,	
Items	AAU	Juelich	AAU	Juelich
$\delta\nu_{10}$	0.202 +/- 0.22	0.218 +/- 0.22	*	0.211
n_{10}	3.07 +/- 0.22	2.84 +/- 0.22	_	_
$\delta\nu_{21}$	0.172 +/- 0.19	0.180 +/- 0.18	0.182 +/- 0.08	0.188 +/- 0.09
n_{21}	3.60 +/- 0.19	3.43 +/- 0.18	3.41 +/- 0.08	3.29 +/- 0.09
$\delta\nu_{32}$	0.152 +/- 0.15	0.157 +/- 0.15	0.167 +/- 0.09	0.171 +/- 0.09
n_{32}	4.09 +/- 0.15	3.96 +/- 0.15	3.70 +/- 0.09	3.62 +/- 0.09
$\delta\nu_{43}$	0.137 +/- 0.16	0.147 +/- 0.17	_	_
n_{43}	4.52 +/- 0.16	4.23 +/- 0.17	_	_
n_{av}	3.82 +/- 0.09	3.61 +/- 0.09	3.55 +/- 0.06	3.45 +/- 0.06
E_g^{opt}	1.73 +/- 0.29 (1.91 eV-2.15 eV)	1.76 +/- 0.33 (1.91 eV- 2.15 eV)	1.69 +/- 0.40 (1.91 eV-2.15 eV)	1.72 +/-0.45 (1.91eV-2.15eV)

In Fig. 4.18 the Tauc's plots for the n- layer to determine the optical gap from the extrapolaton of $(\alpha nE)^{1/2}$ versus E are displayed. The refractive index from the room temperature transmittance data obtained in the two laboratories is used. The two plots have a similar trend except for the extension of their linearity range. For the data from the AAU laboratory the linearity range extends from 1.87 eV to 2.20 eV while for the data from that of the Juelich laboratory it extends from 1.84 eV to 2.30 eV. The optical gap determined from the data obtained in both laboratories are the same with in the value of ($\pm$ 0.03 eV).

This is seen using the values of refractive indices obtained from both reflectance and transmittance spectra of the n- layer.

4.4.4 The Thin i- Layer

In Fig. 4.19 the Tauc's plots for an approximately 100 nm thick intrinsic layer of a-Si : H is displayed. Unlike the thicker samples (approximately ten times thicker) the optical gap is determined from the extrapolaton of $(\alpha E)^{1/2}$ versus E.

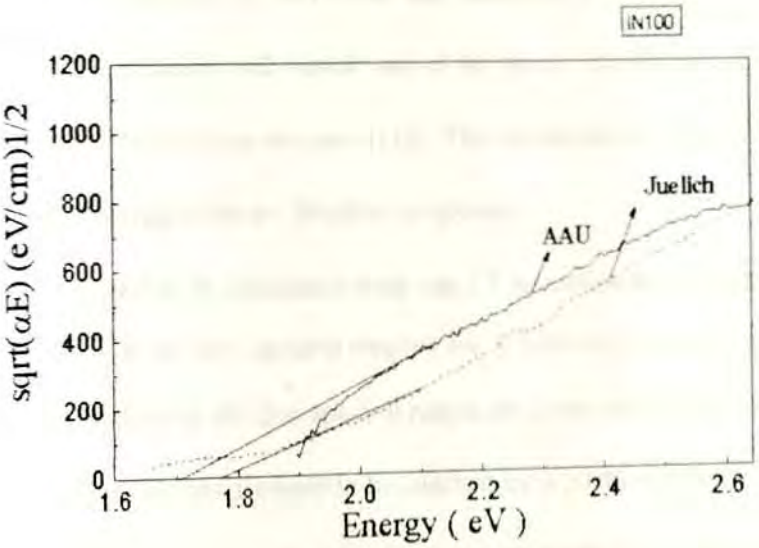

Fig. 4.19 Tauc's plot for approximately 100 nm thick i- layer of a-Si : H.

The two plots have a similar trend except for the extension of their linearity range. For the data from the AAU laboratory the linearity range extends from 1.94 eV to 2.57 eV while for the data from that of the Juelich laboratory it extends from 2.08 eV to 2.93 eV. The optical gap is determined in the extrapolation range of (1.93 eV - 2.27 eV) for the data obtained from the AAU laboratory and in the extrapolation range of (1.97 eV- 2.27 eV) for that

obtained from the Juelich laboratory. The optical gaps determined in these extrapolation ranges are 1.75 +/- 0.35 eV and 1.83 +/- 0.18 eV respectively.

4.5 Accuracy of the Method Used

Each of the interference fringes in the reflectance or transmittance spectra of the samples have a Gaussian distribution with mean position characterized by their maximum. The half width of their distribution is taken to be the full width of the distribution at the half of its maximum value. It is denoted by full width half maximum (FWHM). This value is then taken roughly as the accuracy with which each of the given interference maximum's in their corresponding spectra have been measured [19]. The determination of the FWHM is done by using the Microcal Origin software Window programm.

The refractive index n, is calculated using eqn.2.7 in section two which is the ratio of a constant value $\frac{0.62}{d(\mu m)}$ to the free spectral ranges ($\delta\nu_{ij}$), between two successive interference fringes, where the values of the free spectral ranges are given in terms of energy in the units of eV. Indeed, the finesse has assumed to be constant for a particular measurement. Thus the errors on the spectral free ranges gives the fractional errors on each of the refractive indices determined from them and hence the accuracy with which the refractive indices are measured.

The Tauc's plots, for the determination of the optical gap E_g^{opt} of the samples, have a least squares straight line fit [19] in the energy ranges which are considerd to be highly absorbing regions.

In Tauc's approch the optical gap is determined by extrapolating the plot to the zero ordinate. But the determination depends on the energy range of extrapolation [21]. Different values can be obtained for different ranges of extrapolation. By defining the extrapolation range the Microcal Origin software window programm for fitting curves fits a straight line

and displays the intercept on the ordinate axis, the number of data points lying on the fitted line, and the standard deviation (assuming a common error for the data points scattered about the fitted line) of the measured data points from the fitted line. The accuracy with which the intercept of the fitted line on the ordinate axis is determined is then taken to be the accuracy of the optical gap determined from the extrapolation of the Tauc's plot to the zero value of the ordinate axis.

5. DISCUSSION

The results of the measurements done in the AAU and the Juelich laboratories are already described in section four. In this section the similarities and the differences of the obtained results are discussed. In addition, the possibility of using the investigated a-Si : H thin film samples as component layers for a solar cell structure is discussed.

5.1 Reflectance Measurements

5.1.1 Comparison between Samples of the Same Thickness

In section 4.1 the reflectance spectra of the p-, i-, and n- layers of a-Si : H with an approximately 1000 nm thickness as measured in the two different laboratories at room temperature are displayed.

These samples show more reflectance maxima than the thinner sample (100 nm thick i- layer). However, the number of reflectance maxima are different for the different samples. The i- , p-, and n- layers have 8, 6, and 5 maxima's respectively. This is because of the broadness of the interference fringes. The n- layer has the broader interference fringe width (up to $\Delta\nu$ = 0.16 eV) compared to the p- layer (up to $\Delta\nu$ = 0.13 eV) and the i- layer (up to $\Delta\nu$ = 0.12 eV). These differences are attributed to the differences in the refractive indices between the different samples. The sample with the broader interference fringe has a smaller refractive index. This result is consistent with equations relating the refractive index and thickness of the sample in question to the width and the finesse of the interference fringe. Keeping the finesse to be constant for a given measurement, the interference fringe width $\Delta\nu$, is inversely proportional to the product of the refractive index n, and the thickness d, of the sample (eqn. 2.8 in section two). It also explains why the widths of the interference fringes of a given sample are broader at lower energies.

The refractive index of a medium, which is the ratio of the speed of light in vacuum ($3 \times 10^8 \frac{m}{s}$) to that in a given medium [4] is spectral dependent. It is small for long wavelength light (lower energies). The method used for determining the refractive index at energies where the R or T maxima are seen is rather straightforward. Different values of refractive indices for the same sample are obtained in the two different laboratories. This is due to the inhomogeneous layer thickness at the spot of illumination while the same nominal thickness is used for the determination in equation (eqn. 2.7). Nevertheless, its effect on the optical gap determination is negligible (see Tables 4.10 - 4.12.).

The amplitudes of the reflectance maxima are decreasing from lower to higher energies. This decrease is relatively large at higher energies, on the average in the range (1.6 eV - 2.2 eV). This is the energy region where hydrogenated amorphous silicon has relatively high absorption. The above explanations are equally valid for the measurements done in the two laboratories at room temperature.

5.1.2 Comparison between Samples of Different Thickness

The effect of the thickness of a sample on the optical functions is seen best when comparing the intrinsic layers of thickness 1000 nm and 100 nm. The reflectance spectra of the two samples as measured in the two laboratories are displayed in the figures (Fig 4.2 and Fig. 4.3) of section 4.1.

Unlike the thicker layer the thinner layer of a-Si : H has only one maximum with a broader interference fringe half width (0.63 eV).

The maximum of interference of light by multiple reflections from the thin film samples occur when the optical path difference between successively reflected rays satisfies the condition for the constructive interference (eqn. 2.4). As it is seen in Fig. 4.3 for the thinner film, the condition is satisfied at one particular wavelength and interference order.

Since the samples have the same refractive index, again refering to (eqn. 2.8), the smallness of the sample thickness has given rise to broader interference fringe width (0.63 eV) compared to that of the thicker (up to 0.12 eV).

5.2 Transmittance Measurements

In relatively non absorbing regions of the thin film R and T are complementary, they add up to one [28]. Therefore, what is stated in section 5.1 for the reflectance measurements can equally hold true for the transmittance measurements in the relatively non-absorbing regions. These are the regions where the amplitudes of reflectance or transmittance maxima in their corresponding spectra are relatively large.

However, in the highly absorbing regions, light penetrates only a small depth so that a significant part of the incident light is returned. The transmittance in this regions is too small and it approches a zero value if the layer is thick enough in comparison to the penetration depth of the incident light energy. The reflectance in this region (on the average above 2.25 eV) has a tendency to increase. This energy can be taken as the higher energy limit above which no transmittance have been detected by the photodiode. All the light above this energy range is completely absorbed.

Transmittance is strongly related to the absorption coefficient and penetration depth of the semiconducting film [12]. The decrease in the amplitude of the transmittance maxima of the thicker films, which is relatively high in the energy range (1.6 eV- 2.25 eV) is because of the relatively high absorption coefficient ($\alpha \geq 10^4 cm^{-1}$) of a-Si : H in this range.

The number of maxima in the transmittance spectra are smaller than that in the reflectance spectra of the corresponding layer. The ones which are above 1.9 eV are missing . This is because of the absorption in the layers in this energy range so that the transmittance maxima are relatively very small to have appreciable amplitudes in the spectra.

5.3 Comparison between Measurements Done in the Two Laboratories

5.3.1 Reflectance Measurements

In the reflectance spectra of the samples investigated, (Fig. 4.1- Fig. 4.4) there is a difference in periodicity of their maxima with respect to each measurement done in the two laboratories at room temperature. This periodicity difference in the maxima or minima is originated from the difference in the layer thickness within the illuminated spot on the same samples investigated in the two laboratories. Different layer thickness at the illumination spot will have different energy values for the condition of constructive interference to be satisfied, hence different spectral positions for the maxima or minima. This can be seen by comparing the free spectral range $\delta\nu$,a quantity which can be directly measured from the R or T spectra. For instance, for the p- layer the free spectral ranges of the interference fringes as obtained from the AAU laboratory are slightly smaller than those obtained from the Juelich laboratory. This shows the film thickness of the p- layer at the illumination spot of the reflectance measurement in the AAU laboratory is slightly thicker than the film thickness at the illumination spot investigated on the same sample in the Juelich laboratory.

The ratio of the free spectral range $\delta\nu$, to the full width half maximum (FWHM) $\Delta\nu$, measures the fine-ness or " finesse " of interference fringes (eqn. 2.8). The coefficient of finesses for adjacent interference fringes which corresponds to the measurements done in the two laboratories are given in Table 5.1. Finesse depends on the layer thickness within the R or T illumination spot. Different illumination spots on the same sample can give rise to a different value of finesse due to inhomogeneous film layer thickness. The area under illumination for the reflectance measurement in the AAU laboratory was ~10.4 mm^2 while in Juelich it was approximately 0.0314 mm^2. When the area of the illumination is very large the

probability of encountering a varying film thickness increases and hence the coefficient of finesse decreases which shows a decrease in the spectral free range.

Table 5.1 Coefficient of finesse N_f, half width maximum $\Delta\nu$, and free spectral range $\delta\nu$, for the adjacent interference fringes in the reflectance spectra of each of the samples as calculated from the data taken from the two laboratories.

a) p- layer. b) thick i- layer. c) n- layer.

a)

AAU			Juelich		
$\Delta\nu(eV)$	$\delta\nu(eV)$	N_f	$\Delta\nu(eV)$	$\delta\nu(eV)$	N_f
0.13	0.176	1.35	0.14	0.201	1.43
0.1	0.16	1.6	0.12	0.211	1.75
0.11	0.146	1.33	0.11	0.167	1.51
0.08	0.141	1.76	0.09	0.157	1.74
0.07	0.118	1.68	0.08	0.133	1.61

b)

AAU			Juelich		
$\Delta\nu(eV)$	$\delta\nu(eV)$	N_f	$\Delta\nu(eV)$	$\delta\nu(eV)$	N_f
0.1	0.129	1.29	0.1	0.125	1.25
0.12	0.116	0.96	0.09	0.12	1.33
0.09	0.106	1.17	0.09	0.116	1.28
0.09	0.102	1.13	0.07	0.107	1.51
0.06	0.093	1.55	0.06	0.088	1.31
0.06	0.084	1.4	0.05	0.088	1.76
0.04	0.092	2.3	0.06	0.88	1.31

c)

AAU			Juelich		
$\Delta\nu(eV)$	$\delta\nu(eV)$	N_f	$\Delta\nu(eV)$	$\delta\nu(eV)$	N_f
0.16	0.202	1.26	0.18	0.218	1.21
0.15	0.172	1.32	0.13	0.18	1.38
0.12	0.152	1.26	0.12	0.157	1.31
0.09	0.137	1.52	0.09	0.147	1.63

The amplitudes of the reflectance maxima in the reflectance spectra of all the same samples as measured in the AAU laboratory are different from that measured in Juelich. These differences in the amplitudes are negligibly small in the relatively high absorbing regions. These differences arises because of the type of reference mirror used for the normalization of the reflectance measurements.

The type of mirror used to normalize the reflectance measurements of the samples in the AAU laboratory was an uncalibrated commercial glass mirror. In the Juelich laboratory they have used an aluminum mirror which was calibrated with a standard reflector. Because of this difference in the type of mirror used, the reflectance amplitudes of the same samples are different. The amplitudes in the reflectance spectra of the samples as measured relative to the glass mirror (used in the AAU laboratory) are generally larger than the amplitudes in the reflectance spectra of the same samples as measured in Juelich.

5.3.2 Transmittance Measurements

In the transmittance spectra of the samples (Fig. 4.6 - 4.9) like in that of the reflectance spectra, there is a periodicity difference in their transmittance maxima with respect to each of the measurements done in the two laboratories.

The reasons which are given for the periodicity difference of the reflectance maxima in the reflectance spectra of the given sample with respect to the measurements done in the two laboratories can also explain the periodicity difference of the transmittance maxima in their transmittance spectra. The coefficient of finesse N_f, the half width maximum $\Delta\nu$ and the free spectral range $\delta\nu$, for the adjacent interference fringes which corresponds to measurements done in the two laboratories are given in Table 5.2. The slight differences in their free spectral ranges in the transmittance spectra of the same samples as measured in the two laboratories are again arise from inhomogeneous film layer thickness. The free spectral

ranges of the p- and n- layers as measured in the AAU laboratory are slightly smaller than that measured in the Juelich laboratory showing a slightly thicker film layer thickness of each layer at the illumination spot of their transmittance measurement in the AAU laboratory in comparison to that in the Juelich laboratory.

Table 5.2 Coefficient of finesse N_f, half width maximum $\Delta\nu$, and free spectral range $\delta\nu$, of adjacent interference fringes in the transmittance spectra of each of the samples as calculated from the data taken from the two laboratories.

a) p - layer. b) thick i - layer. c) n - layer.

a)

AAU			Juelich		
$\Delta\nu(eV)$	$\delta\nu(eV)$	N_f	$\Delta\nu(eV)$	$\delta\nu(eV)$	N_f
0.07	0.184	2.62	0.08	0.218	2.72
0.06	0.166	2.76	0.07	0.203	2.9
0.06	0.155	2.58	0.07	0.18	2.57
0.05	0.14	2.8	0.07	0.162	2.31

b)

AAU			Juelich		
$\Delta\nu(eV)$	$\delta\nu(eV)$	N_f	$\Delta\nu(eV)$	$\delta\nu(eV)$	N_f
0.04	0.122	3.05	0.04	0.128	3.2
0.03	0.108	3.6	0.04	0.113	2.828
0.04	0.109	2.725	0.04	0.112	2.8
0.03	0.091	3.03	0.03	0.099	2.3

c)

AAU			Juelich		
$\Delta\nu(eV)$	$\delta\nu(eV)$	N_f	$\Delta\nu(eV)$	$\delta\nu(eV)$	N_f
0.06	0.182	3.03	0.07	0.188	2.68
0.06	0.163	2.78	0.06	0.171	2.85

Here too, there are amplitude differences between the maxima in the transmittance spectra of each of the samples as measured in the two laboratories. In the AAU laboratory, the light transmitted through the base substrate (Corning glass) has been used for normalization of

the transmittance measurements while in Juelich the reference has been the direct light incident on the sample. This difference in the reference light intensity used in the transmittance measurements of the samples in the two laboratories is responsible for the observed amplitude differences in the corresponding transmittance maxima. The glass substrate is not totally transparent and the transmittance of the samples measured relative to the transmittance through the glass, as in the AAU laboratory, have higher amplitudes in comparison to that from the Juelich laboratory which is measured relative to the direct incident light intensity.

5.3.3 The Absorption Coefficient, α

The absorption coefficient, given in the logarithmic scale versus the photon energy for each of the samples is shown in the figures (Fig. 4.9 - 4.12). Each plot shows the spectral dependence of the absorption coefficient in the absorbing regions as measured in the two laboratories at room temperature. With increasing energy they all show a steep increase in absorption followed by a gradual increase and then a uniform absorption character.

The absorption coefficient values of each of the samples obtained for the data from the AAU laboratory is higher than or equal (thick i- layer) to that obtained from the Juelich laboratory in the energy ranges which are on the average below 2.35 eV. There are some parts in the energy range of the relatively medium absorbing regions (regions over which interference fringes with relatively small amplitudes are seen in their T spectra) where interference structures are seen in the absorption spectra. The maxima seen in this energy region of the spectra have relatively higher amplitudes as compared to that of the measurement done in the Juelich laboratory.

It was mentioned in section 5.3 that transmittance is strongly related to the penetration depth of the illuminating light and the absorption coefficient. This can also be seen from the

Hishikawa's relation (eqn.2.9) which is used for the determination of the absorption coefficient. In Hishikawa's relation the term T / 1-R makes the determination free of interference structures [30]. But this is true if and only if T and R are measured at exactly the same position on the sample. If the two spots on a given sample at which R and T are measured are identical, then no error is caused on the measurement due to variation in film thickness over the inhomogeneous film layer. In this case T / 1- R is free of interference fringes. The interference structures seen in the absorption spectra of the samples as determined in the two laboratories are caused due to the difference in the spot of illumination for the R and T measurement on these samples which have inhomogeneous film layer thickness. The relatively large amplitudes in the interference structure of the absorption spectra obtained from the AAU laboratory in comparison to that obtained from the Juelich laboratory shows that there is a relatively large difference on the spot of illumination for the R and T measurement of the same samples in the AAU laboratory. This is mainly caused from the large area of illumination for the measurement done in the AAU laboratory ($\sim$10.4 mm^2) in comparison to that in Juelich ($\sim$ 0.0314 mm^2) in which case the probability of encountering varying film layer thickness is relatively small.

The spectroscopic set up used for the measurements done in the AAU laboratory has an additional effect on the R and T measurements hence an additional cause for the observed interference structure on the absorption spectra. The sample and the reference sample for the reflectance measurements or the transmittance measurements were not placed on the sample holder at same time. The samples and the reference sample are placed one after another. But in doing so the angular position of the sample holder would be changed and hence the angle at which the reflected or transmitted light beam hits the grating in the monochromator. Thus the spectral positions of the maxima in the reflectance spectra and the minima in the

transmittance spectra will not coincide and giving rise to interference structure in the absorption spectra.

The higher absorption coefficient values obtained from the AAU laboratory with respect to that obtained from the Juelich laboratory are due to the difference in the actual spot of illumination on the same samples and hence a different layer thickness for their corresponding R or T measurements. The higher absorption coefficient values shows that a slightly thicker layer thickness at the actual spot is illuminated on each of the same samples except for the thicker i- layer in the R or T measurements done in the AAU laboratory in comparison to that in Juelich.

The absorption coefficient values of the thicker i- layer are more than an order of magnitude higher than those of the thin i- layer as it is measured in the two laboratories. This is because of relatively small thickness of the thin i- layer compared to the penetration depth of the illuminating light.

5.3.4 The Optical Band Gap, E_g^{opt}

The optical energy band gap for the thicker films are determined from the extrapolation of the plot of $(\alpha nE)^{1/2}$ versus energy to zero ordinate. The refractive indices from the reflectance measurements in the two laboratories are used in the figures (Fig. 4.13, 4.15, 4.17) while in the figures (Fig. 4.14, 4.16, 4.18) the refractive indices obtained from transmittance measurements are used. Since the abscissa in the Tauc's plot contains the spectral dependent optical constants α , and n, all the effects seen in their determination will contribute to the optical band gap determination.

The difference in the amplitudes of maxima in the relatively medium absorbing regions can be explained by what is stated for the absorption coefficient values in section 5.3 because these plots are only transformations of the absorption spectra. In addition to what is seen in

the absorption spectra, the refractive index n, has an additional effect for the apparent shift of the Tauc's plot of each of the samples to higher values with respect to that obtained from Juelich. Again these differences in the refractive indices of the same samples as obtained in the two laboratories arises from the difference in the actual illuminated spots of each of the same samples.

The method used to determine the refractive indices from R or T maxima is not reliable specially at higher energies because there the R or T maxima is affected by absorption in the thin film.

The transmittance and reflectance spectra of a given sample may give rise to different values of the refractive indices (see Tables 4.10 - 4.12) due to the rare possibility of illuminating identical spots for both reflectance and transmittance measurement on a non-homogeneous sample. These different values of refractive indices may give rise to different values for the optical gap of a given sample. A difference in the optical gap determination (up to $\pm$ 0.04 eV, $\pm$ 4%) is obtained for the measurement done in both laboratories by using refractive indices obtained from R and T spectra. This difference is not significant and it is in the limit of the experimental determination.

Depending on the energy range used for extrapolation, especially the lower end of the energy range, significant differences in the optical energy gap determination can be obtained for a- Si : H. As long as Tauc's approach of the optical gap determination employs relatively low energy R and T data centered on $\alpha = 10^4 cm^{-1}$ [21] , the optical gap determined from R and T data from the AAU laboratory and the Juelich laboratory have a difference (up to 0.04 eV). This is because mainly of the differences in the film layer thickness at the actual illuminated spots of measurements of each of the same samples investigated in the two laboratories.

For the thin i- layer the optical gap is determined from the extrapolation of the $(\alpha E)^{1/2}$ versus energy plot to the zero ordinate. Here n is not included in the determination. A difference (up to 0.05 eV) is seen for the data from the AAU laboratory while a difference of ~ 0.1 eV is obtained from that of the Juelich laboratory if n from reflectance or transmittance spectra is included. Therefore, these differences are only due to the differences in the absorption spectra. However, this difference in the absorption spectrum, for a given sample of different nominal thickness has negligible effect on the optical gap determined from Tauc's plot.

In the determination of the optical gap of the i- layer from the data obtained from the two laboratories a difference of (~ 0.08 eV) is seen differing from optical gap value obtained when n, from the transmittance spectra is included which is (~ 0.01 eV). Again this arises from the difference in the film layer thickness at the actual illuminated spot of measurement on the same sample. The relatively large difference in the optical gap determined in the two laboratories for the thinner layer arises from relatively large difference in the actual film layer thickness at the illumination spot of measurement in the two laboratories.

5.4 Possibility of Using the Sample Layers as a Solar Cell Component

The p- i- n junction structure was the assumed solar cell structure and a typical structure of amorphous silicon p- i - n solar cell is shown in section two (Fig. 2.2) where the light enters the solar cell along the p- side. When light falls on a semiconducting film, part of it (light with photon energies greater than the band gap energy E_g, of the film) will be absorbed while part of it, light with photon energies less than E_g , will be transmitted through it [11,12].

The p- layer has comparatively wider optical gap (1.79 eV) than the i- layer (1.70 eV) and the n- layer (1.73 eV). To pass much of the incident light where it is collected, the intrinsic layer, light should enter through the p- side. Thus the p- side has a window effect.

The p- layer of a- Si : H as measured in the AAU laboratory has an optical gap of E_g^{opt} = 1.79 eV. But its window effect is only for photons with an energy less than 1.79 eV in which case only part of the light in the near infrared of the visible light spectrum will pass through the p- layer and then to the i- layer where it is needed to be collected. The solar spectrum on the earth's surface has a relatively large spectral irradiance in the visible range [12, 22]. The maximum occurs in the green. Thus there will be a loss in the photogeneration due to incomplete absorption of the incident light energy in the visible range of the spectrum. For this reason a p- layer with a relatively wider optical band gap is needed so that there will be no loss even at the blue end of the spectrum. P- layers of a- Si : H with an optical gap E_g^{OPT} = 1.92 eV determined from Tauc's approach, which would be much more efficient have been reported [6, 16].

The n- layer has an optical gap E_g^{opt} = 1.73 eV, which is almost equal to that of the i- layer E_g^{OPT} = 1.71 eV. This enables the light with photon energies less than its energy gap (1.71 eV) not to be absorbed in the n- layer, but transmitted through it. A suitable reflecting material, which is also acting as an ohmic contact can reflect the photons back again through the n-layer so that they ultimately reach the i- layer for another probable chance of collection.

The loss of the carriers which could be generated by part of the visible light spectrum incident on the solar cell and the long wavelength light, in particular those just above the band gap edge of a -S i : H will reduce the short circuit current I_{sc}, and the open circuit voltage V_{oc}. These will reduce the efficiency of the solar cell.

6. CONCLUSION

Based on room temperature reflectance and transmittance measurements the optical functions for glow discharge produced a - Si : H thin films have been obtained over the energy range 1.24 eV < E < 3.54 eV. These measurements, on the same samples were also performed previously by Ato Challa Bekele [29] in the laboratory of ISI - PV in Forschungszentrum, Juelich (Germany) and are presented in this work for comparison.

The optical spectra of each of the samples obtained in the two laboratories show the same trends except from the periodicity differences in the maxima or minima and amplitude differences with respect to each of the corresponding measurements. These differences are attributed to : a) the different reference samples used for the normalization of the reflectance or transmittance measurements b) the different spots of illumination on a given sample whose thickness is inhomogeneous c) the lack of adequate condensing optics in the spectroscopic setup for the measurement done in AAU.

These differences have an effect on both optical functions α and n which in turn affect the optical gap determination. However, the same optical gap values within the value (up to $\pm$ 0.04 eV) are obtained from the measurements done in the two laboratories.

A purely homogeneous film surface or a comparatively small illuminating spot size on a sample, such that ideally a homogeneous surface is illuminated, could reduce these differences. A better optical bench, which makes the real near normal incidence reflectance possible and adequate condensing optical components would provide a better result.

The possibility of the measurement of optical constants in the Addis Ababa University Department of Physics, is verified for the first time.

REFERENCES

[1] Aruan Maden, Melvin P. Shau, The Physics and Application of Solar Cells,Glasstech. Solar Inc., Wheatridge, Colrado (1988)

[2] M. H. Brodsky, Topics in Applied Physics, Springer, Berlin, volume 36 (1985)

[3] SPIE, vol.763, Physics of Amorphous Semiconductor Devices (1987)

[4] David Adler, Brain B. Schwarth and Martin C. Steele, Physical Properties of Amorphous Materials, Institiute for Amorphous Studies Series (1985)

[5] Yoshiro Hamakawa, Solar and Wind Technology, vol.6. No. 3, pp. 235 - 240 (1989)

[6] Yoshiro Hamakawa, Solar and Wind Technology, vol.6. No. 3, pp. 241 - 246 (1989)

[7] Walter A. Harrison, Solid State Theory, Dover Publications, Inc., New York (1979)

[8] Euro Catalogue, Oriel Corporation, volume II.

[9] Aruan Maden, Solar and Wind Technology vol. 5. pp. 473 - 487 (1988)

[10] Larry D. Partain, Solar cells and Their Applications, John wiely & Sons, Inc., New York (1995)

[11] S.M.Sze, Physics of Semiconductor Devices, Wiely Interscience, New York (1969)

[12] Donald A. Neamen, Semiconductor Physics and Devices, Richard D. Irwin, Inc. (1992)

[13] Jack L.Stone, Physics Today, September, 1993 pp. 22-29

[14] Martin A. Green, Keith Emery, Klaus Bucher and David L. King, Progress in Photovoltaics, vol. 3. No.1, pp. 51- 55 (1995).

[15] Thomas Markvart , Solar Electricity, John Wiley & Sons Ltd., England (1994)

[16] Amensisa Abdi, Thesis (AAU), Optical Characterization of Thin Films for Solar Cell Application (1994)

[17] O.S. Heavens, Optical Properties of Thin Solid Films, Dover Publications Inc., New York (1965)

[18] K. D. Leaver and B.N. Chapman, Thin Films, Wykeham Publications Ltd. London (1971)

[19] Louis L., A Practical Guide to Data Analysis for Physical Science Students, Cambridge University Press, New York (1991)

[20] M.R.I. Ramadan, Solar and Wind Technology vol. 6 No.5 pp.615 - 618 (1989).

[21] R.M Dawson, Mat. Res. Soc. Symp. proc. vol. 258. pp. 595- 600 (1992)

[22] H.Schade and Z.E.Smith., J. App. Phys. vol. 57 pp. 568 (1985)

[23] W.Demtroeder, Laser Spectroscopy, Springer, Berlin (1993).

[24] Anne P. Thorne, Spectrophysics, ELBS edition Champman and Hall Ltd., London, 2 nd edition (1987)

[25] Joachim Herrmann, Bernd Wilhelmi; Laser for Ultrashort Light Pulses, Revised translation of Laser fur Ultrakurze Lichtimpulse, North - Holland (1987)

[26] Marcelo Alonso, Edward J. Finn; Fundamental University Physics, volume II, Fields and Waves, Addison - Wesley world student series edition, sixth edition (1974)

[27] Wim C. Sinke, Guest editor; MRS Bulletin, A Publication of the Materials Research Society,October 1993, volume 18, No. 10 pp. 18 - 21.

[28] C. N. Banwell, Fundamentals of Molecular Spectroscopy, 2nd edition, Mc Graw-Hill, England (1972)

[29] Challa Bekele, Thesis (AAU), Temperature Dependence of the Optical Properties of a-Si : H Thin Films for Solar Cells (unpublished).

[30] N.Maley, Jpn. J. Appl. Phys. vol.31. No.3, pp. 768-769 (1992)

DECLARATION

I, the undersigned, declare that my thesis being entitled is my original work and has not been presented for a degree in any other University. Sources of relevant materials taken from books and articles have been duly acknowledged.

Name : Endeshaw Bekele

Signature :----------

Place and date of submission : Addis Ababa University, Department of Physics, June 1996.

This thesis has been submitted for examination with my approval as University advisor.

Name : Dr. Ulrich Stutenbaeumer

Signature :----------

Date : 26.06.96